Aus dem Institut für Biosynthese Neuraler Strukturen

des Zentrums für Molekulare Neurobiologie Hamburg

des Universitätsklinikums Hamburg-Eppendorf

Prof. Dr. Melitta Schachner

Stereological analyses of neurons and glial cells
in the lesioned and unlesioned spinal cord
of wild-type and CHL1-deficient mice

Dissertation

zur Erlangung des Grades eines Doktors der Medizin

dem Fachbereich Medizin der Universität Hamburg

vorgelegt von

Ayşe Acar

aus Hamburg

Hamburg 2009

Angenommen vom Fachbereich Medizin der Universität Hamburg am: 04. Januar 2010

Veröffentlicht mit Genehmigung des Fachbereichs Medizin der Universität Hamburg

Prüfungsausschuss, der/die Vorsitzende: Prof. Dr. Schachner

Prüfungsausschuss, 2. Gutachter/in: PD Dr. Irintchev

Prüfungsausschuss, 3. Gutachter/in: Prof. Dr. Glatzel

CONTENTS

1 INTRODUCTION

1.1 Spinal Cord Injury

The limited regeneration potential of the mammalian spinal cord is a serious challenge for medicine and science. The lack of regenerative ability is explained with injury-induced changes in neurons, on one side, and, on the other, with changes in the environment at the site of injury. Elucidation of the complex pathophysiology of the spinal cord injury (SCI) and experimental manipulations of this environment attract research interest because of the opportunity to create conditions beneficial for neuronal regeneration.

1.1.1 Epidemiology of spinal cord injury

SCI is a traumatic lesion of neural elements in the spinal cord, resulting in any degree of sensory or motor deficit, automatic dysfunction and bladder or bowel dysfunction. The injury can be blunt or penetrating trauma. Worldwide, an estimated 2.5 million people live with SCI, with more than 130,000 new injuries reported each year (Thuret et al., 2006). The annual incidence of SCI varies between 12 and 58 cases per million people in different countries (Martins et al., 1998; Tator, 1995, 2000).

In comparing the causes for SCI, there is a lack of uniformity between the countries and even within the countries (Ackery et al., 2004). Several trends in the etiology of SCI were identified: motor vehicle collisions were the leading cause of SCI in developed countries (58%) (Martins et al., 1998), falls are the second leading cause (47%) (Krassioukov et al., 2003; O'Connor, 2002). In developing countries falls and incidents due to violence are the leading cause in the incidence of SCI (da Paz et al., 1993; Dincer et al., 1992; Fazlul Hoque et al., 1999; Hart et al., 1994).

The highest incidences of SCI, regardless of country, were reported in persons between 20 and 40 years of age (Ackery et al., 2004). In males, SCI is more prevalent than in females (Bracken et al., 1981; Sekhon et al., 2001; Tator et al., 1993), the male-to-female ratio is approximately 3-4 to 1.

Because SCI most commonly affects young and healthy individuals, it is not only an enormous cost to individuals, but also a significant financial burden to society. The Center for Disease Control estimated that the United States spends $9.7 billion ($US) on the treatment of SCI each year (2003). Overall costs per SCI patient are estimated to exceed $1 million (McKinley et al., 1999). Information about the cost of SCI in less

developed countries is limited, moreover these countries do not have resources to support SCI patients (Levy et al., 1998).

1.1.2 Pathophysiology of spinal cord injury

Injuries like contusion, compression, penetration or maceration of the spinal cord can disrupt the normal architecture of the human spinal cord (Bunge et al., 1993; Kakulas, 1999). After SCI, there is a massive cell death of neurons, oligodendrocytes, astrocytes and their precursor cells at the lesion site. Vascular trauma caused by mechanical forces leads to the disruption of the blood brain barrier and disturbances in circulation leading to hypoxia. Parenchymal and vascular damage cause secondary loss of neurons and glial cells, and activation of classical inflammatory and wound healing responses (Velardo et al., 2004). Inflammatory cells have a range of destructive and reparative roles after SCI many of which, however, are still poorly understood (Jones et al., 2005). The cell death causes cavities and cysts which interrupt descending and ascending axonal tracts (Crowe et al., 1997). Secondary processes like ongoing apoptosis of oligodendrocytes and loss of myelin lead to a secondary loss of function (Thuret et al., 2006). A characteristic feature of the reparative process after SCI is glial scarring, a multifactorial process that involves reactive astrocytes, glial progenitors, microglia and macrophages, fibroblasts and Schwann cells (Thuret et al., 2006). The glial scar, built mainly of the reactive astrocytes, prevents further inflammation and neurodegeneration (Bush et al., 1999; Faulkner et al., 2004), but at the same time it is a barrier which hinders axonal regeneration via numerous growth-inhibiting molecules (for review see Silver and Miller, 2004). Whereas the cellular composition, molecular expression and evolution of the glial scar at the lesion site are well characterized, there is sparse, and largely controversial knowledge about the changes in numbers of neurons and glial cells in the spinal cord caudal to the lesion site. For example, both neuronal cell loss and lack of it have been reported for distal spinal cord segment (Young, 1966; Eidelberg et al., 1989; McBride and Feringa, 1992; Bjugn et al., 1997). Also, the alterations in glial populations, including increase in densities of microglia and astrocytes, as well as loss of myelin-forming oligodendrocytes in distal segments of CNS upon injury have been reported (Holmes, 1906; Gledhill and McDonald, 1977; Harrison and McDonald, 1977; Landis, 1994; Schwab and Bartholdi, 1994; Streit et al., 1999). Many questions about glial cells after injury still remain open, for example, to which extent proliferation of oligodendrocyte progenitors compensates for myelin loss,

if there is a significant proliferation or just activation of the astrocytes, if microglia proliferates *in situ* or is mainly blood-derived (Schwab and Bartholdi, 1994).

Repair after SCI also includes proliferation of ependymal and peri-ependymal canal precursor cells and their differentiation into glial cells (Beattie et al., 1997; Yang et al., 2006; Yamamoto et al., 2001; Azari et al., 2005). Axon sprouting is also seen, however only a few axons regenerate over long distances to their original targets (Hill et al., 2001). New spinal circuits are built to bypass the lesion (Bareyre et al., 2004; Raineteau et al., 2002), cortical sensorimotor areas can functionally rearrange (Raineteau et al., 2001; Bareyre et al., 2004) and the rubrospinal system can reorganize and compensate for much of the function lost (Raineteau et al., 2001).

1.1.3 Therapy

The spontaneous repair after SCI is not complete and interminable. There are no fully restorative therapies for SCI yet, but many interventions are now in, or moving towards, clinical trials.

One of the possible therapeutic strategies is the cellular transplantation with the aims to bridge any cysts or cavities, to replace dead cells and to create a favorable environment for axon regeneration (Thuret et al., 2006). Various molecular therapies are another strategy undergoing trials aimed to protect neurons from secondary cell death, to promote axonal growth and to enhance conduction (Thuret et al., 2006). Up to now, the only efficient ways to improve the locomotor function are exercises and physical rehabilitation therapies, commonly used as a treatment after SCI in humans (Engesser-Cesar et al., 2002). Nevertheless, many SCI patients become paraplegics or quadriplegics suffering lifelong severe disabilities.

1.2 Cell Adhesion Molecules

Cell adhesion molecules (CAMs) are integral membrane proteins with essential functions for the construction of the central nervous system (CNS) architecture like cell migration, cell adhesion, neurite outgrowth, axonal fasciculation and synapse formation. They are a requirement for proper cell-cell interactions and synaptic plasticity, since with their extracellular domains CAMs are able to interact with binding partners in the extracellular matrix or carried by other cells and, thereby, activate signal pathways. These processes are necessary for the proper development of the CNS and its maintenance and function in the adult. Disturbances in these processes lead to severe

human developmental diseases. Moreover, increasing evidence indicate that CAMs play essential roles in repair processes after CNS and PNS damage (Apostolova et al., 2006; Simova et al., 2006; Jakovcevski et al., 2007; Lieberoth et al., 2009)

Cell adhesion molecules are divided into three major families: the integrins, the cadherins and the immunoglobulin superfamily (IgSF). Those CAMs which are most importantly involved in CNS development and function belong to the IgSF which is characterized by the presence of at least one Ig like-domain, enabling them to mediate cell adhesion in a calcium independent manner. All members of the IgSF have characteristic temporal, area- and cell-specific expression patterns (Holm et al., 1996; see Reviews: Rathjen and Jessell, 1991; Schachner et al., 1991, 1994; Rutishauer et al., 1993).

The IgSF is subdivided in three subgroups depending on the number of Ig-like domains, the presence and number of fibronectin (FN) III repeats and the mode of attachment to the cell membrane (Cunningham, 1995). The neural cell adhesion molecule (NCAM), L1 and the close homologue of L1 (CHL1) are members of subgroup 2 containing Ig-like domains and FN III repeats. Both molecules are indispensable for normal brain development and function and are essential for neural regeneration (Dahme et al., 1997; Montag-Sallaz et al., 2003; Chen et al., 2007; Jakovcevski et al., 2007).

1.3 CHL1

CHL1 was discovered when a lambda gtl1 expression library for cDNA clones was screened with L1 polyclonal antibodies (Tacke et al., 1987) with the aim to find cDNA clones containing L1. One of the isolated clones contained a partial cDNA sequence with 34% homology to L1. Subsequently, a full length cDNA clone was isolated encoding a novel protein of 1209 amino acids with a calculated molecular mass of approximately 135 kD (Holm et al., 1996). This new molecule was named close homologue of L1 (CHL1).

CHL1 consists of the same structural elements as the other members of the L1 family, it shares 60% amino acid identity with L1 in the extracellular region and 40% identity in the cytoplasmic domain (hence the name "close homologue"). Expression of CHL1 seems to be restricted to the nervous system (Hillenbrand et al., 1999; Holm et al., 1996). The first expression of CHL1 in mice and rats can be detected at embryonic day 13. Until postnatal day 18, CHL1 levels increase and then start declining

subsequently to low levels in the mature brain except for areas of high plasticity like the hippocampus where it is expressed throughout adulthood (Hillenbrand et al., 1999). While the expression patterns of L1 and CHL1 overlap considerably there is one striking difference in that CHL1 transcripts, but no L1 transcripts, can be found in astrocytes and oligodendrocyte precursor cells (Hillenbrand et al., 1999). Furthermore, CHL1 is expressed by non-myelinating Schwann cells and some neurons in the peripheral nervous system (PNS) (Hillenbrand et al., 1999).

The functional properties of CHL1 have not been as intensively investigated as those of L1. *In vitro* studies have shown that CHL1 is able to promote neurite elongation and neurite survival (Chen et al., 1999). Recent findings suggest an important role of CHL1 in lesioned nervous tissue since CHL1 is strikingly upregulated in Schwann cells and sensory neurons after nerve crush injury (Zhang et al., 2000). Adult neurons of the CNS are also able to up-regulate CHL1 expression after a lesion provided their axons can regrow in a permissive environment like that of a peripheral nerve graft (Chaisuksunt et al., 2000a; Chaisuksunt et al., 2000b).

1.4 CHL1 mutations in humans

Japanese scientists studied the linkage of CHL1 to psychotic diseases (Sakurai et al., 2002). The CHL1 gene (designated also as cell adhesion L1 like, CALL, in humans), located on human chromosome 3p26, was screened for mutations in schizophrenic patients. A missense polymorphism (Leu17Phe) was identified which subsequently led to further examination of the association between the Leu17Phe polymorphism and schizophrenia. It was found that the frequency of leucine at amino acid 17 was significantly higher in patients with schizophrenia. Leu 17 is located in the hydrophobic core region of a signal peptide. Some mutations in the hydrophobic core region of signal sequences have been reported to have a direct correlation with defective protein synthesis and pathological status. The results of this study suggest that the CHL1 protein might be involved in the etiology of schizophrenia. A case-control association study of CHL1 and schizophrenia done in the Chinese population confirmed the positive association (Chen et al., 2005).

1.5 CHL1-deficient mice

In order to find out more about its functions, CHL1-deficient (CHL1-/-) mice were generated (Montag-Sallaz et al., 2002). Analyses with mice lacking the gene for a given molecule provide better insight into the biological functions of these molecules. Furthermore, the "knockout" animals can be seen as adequate models for respective human gene ablations. CHL1 null mutant mouse was generated by disruption of the ribosomal binding site, the translation initiation codon and the amino terminus including the signal sequence (Montag-Sallaz et al., 2002).

In CHL1-deficient mice the gross morphology of most brain regions like thalamus, cerebellum, main fiber tracts and retina do not differ from wild-type mice, only the ventricles are enlarged (Montag-Sallaz et al., 2002). The knockout mice are also viable, fertile and have a normal life span. Their gross sensory functions, reflexes and motor ability are not obviously restricted (Montag-Sallaz et al., 2002). However, few subtle morphological abnormalities have been detected in CHL1-deficient mice. In the CHL1-/- hippocampus, the mossy fibers show path-finding errors within the CA3 region. Only a few thin bundles or single mossy fibers project through the pyramidal cell layer of CA3, instead of being organized in clearly separated supra- and infrapyramidal bundles. This altered projection can affect the converting of area information and therewith explain the abnormal exploratory behavior of CHL1-/- mice (Montag-Sallaz et al., 2002). The olfactory bulb also seems to be affected since olfactory neurons in the CHL1-deficient mouse establish contacts with more than one glomerulus, a condition never observed in wild-type mice. Additionally, some axons in the mutant abnormally pass through the glomerular layer and form contacts within the external plexiform layer (Montag-Sallaz et al., 2002).

A striking finding in the CHL1 mutant mouse is a significant up-regulation of NCAM 180 in the olfactory bulb, the cortex, the hippocampus and the amygdala which are brain regions with high levels of CHL1 expression in the adult wild-type mouse, regions characterized by a high degree of synaptic plasticity throughout life (Montag-Sallaz et al., 2002). These findings demonstrate similar and perhaps overlapping functions of both molecules *in vivo*. Thus, the enhanced expression of NCAM in the CHL1-/- mouse might be indicative for compensatory functions of NCAM.

The pyramidal cells in the neocortical layers are abnormally distributed in CHL1-/- mice (Demyanenko et al., 2004). The alterations are especially striking in the secondary visual cortex (V2 region), a region, in which CHL1 is expressed at the highest level.

Many pyramidal cells are displaced from the fifth into the forth cortical layer and have abnormally orientated apical dendrites. In the somatosensory cortex, the apical dendrites show a waved shape, but the pyramidal neurons are not misplaced. In regions with lower CHL1-expression like the motor cortex, there are no altered or displaced pyramidal cells. These data implicate that CHL1 affects the destination of some neurons and regulates the area-specific navigation of dendrites. These findings were explained by the decrease in neuronal migration, as the migration velocity of neurons in the CHL1-/- mice is reduced to 25% in comparison with the wild-type mice. Because of this decelerated migration, the neurons in adult mice accumulate in the white matter and the ventricular zone. A reason for this defective process can be a reduced adhesion aptitude in the radial glia (Demyanenko et al., 2004).

The influence of CHL1 on the regulation of inhibitory synapses and the number of interneurons has been shown in studies on three-week-old mice (Nikonenko et al., 2006). In CHL1-/- mice, the long-term potential (LTP) - a long-lasting enhancement in communication between two neurons that results from stimulating them simultaneously - in excitatory CA3-CA1-synapses is reduced, since an increased inhibition by perisomatically projecting interneurons takes place. The LTP can be normalized by GABA-antagonists (Nikonenko et al., 2006). In 2- to 3-month-old mice the LTP in CA3-CA1-synapses is normalized. During the postnatal development, the maturation of the GABAergic system in CHL1-/- mice seems to be limited, so that the perisomatic inhibition on CA1 pyramidal cells is reduced (Morellini et al., 2006).

Significant differences between CHL1 mutants and wild-type animals have been observed in the open field paradigm (Montag-Sallaz et al., 2002). The mutants spend more time in the central area, which may indicate reduction of anxiety or a different exploratory behavior. The observation that CHL1-deficient mice have shown significant differences in the Morris water maze as compared to littermates with respect to the path swum parallel to the wall and increased swim path tortuosity, absolute spin, and time spent in the centre quadrant further supports the different exploratory behavior (Montag-Sallaz et al., 2002). Morris water maze is the most popular task in behavioral neuroscience assessing spatial learning and memory in its most basic form. In studies in which CHL1-/- mice are confronted with intruders, the mutants are less aggressive (Frints et al., 2003), but show also less interest in the unknown individual (Morellini et al., 2006).

Behavioral surveys with CHL1-deficient mice have confirmed the coherence between CHL1 and schizophrenia, for the mutants show similar behaviors like schizophrenia patients such as a deficiency of attention or a reduced response to outer stimuli during the negative symptomatic (Morellini et al., 2006).

1.6 CHL1 and regeneration in the nervous system

After injuries of CNS and PNS in adult mice, CHL1 is upregulated in its expression in both neurons and astrocytes (Chaisuksunt et al., 2000; Zhang et al., 2000; Rolf et al., 2003). CHL1 plays an important role in SCI. Jakovcevski et al. (2007) showed that adult CHL1-deficient mice recover better than wild-type mice from compression injury of the spinal cord, indicating that CHL1 has a negative impact on spinal cord regeneration. Upregulation of CHL1 expression induced by basic fibroblast growth factor (FGF-2) in glial scar astrocytes was identified as a possible cause of the inhibitory effect that CHL1 has in regeneration. Furthermore, *in vitro* findings that CHL1 impedes neurite outgrowth when present on both neurons and astrocytes in coculture, and evidence for a homophilic binding mechanism support the idea that CHL1 has dual functions, conductive and inhibitory, depending on its spatial, temporal, and cell type-specific expression (Jakovcevski et al., 2007).

2 RATIONALE AND AIMS OF THE STUDY

Previous work has produced controversial results as to the alterations in neuronal and glial cell populations in the lumbar spinal cord (Young, 1966; Eidelberg et al., 1989; McBride and Feringa, 1992; Bjugn et al., 1997). In addition to use of different models of SCI, like cats, rats or monkeys (Young, 1966; Bjugn et al., 1997; Yang et al., 2006), a reason for the controversies appears to be the application of different, often biased methods for assessment of cell numbers. Here we considered that use of a novel quantitative (stereological) approach based on immunohistochemical visualization of defined cell types might provide novel insights into the pathophysiology of SCI. This method has been established in the Institute and provides the opportunity for simultaneous analysis of all major glial cell types and of chemically-defined subpopulations of neurons (Irintchev et al., 2005).

To evaluate to what degree changes in the size of major neuronal and glial cell subpopulations (e.g. neuronal loss, astrogliosis) in the lumbar spinal cord contribute to the differential outcome of compression thoracic SCI in adult CHL1 deficient mice and wild-type littermates, the following questions were addressed:

- Does injury of the lower thoracic spinal cord of wild-type mice cause alterations in the neuronal and glial cell populations in the lumbar spinal cord compared with intact mice?
- Does injury of the lower thoracic spinal cord of wild-type mice cause an alteration of the volume of the lumbar spinal cord compared with intact mice?
- Does CHL1 deficiency cause alterations in the neuronal and glial cell populations in the intact lumbar spinal cord compared with intact wild-type littermates?
- Do the changes in the neuronal and glial cell populations after SCI differ in CHL1-deficient mice compared with wild-type littermates?

3 MATERIALS AND METHODS

3.1 Animals

Twelve CHL1-deficient (CHL1-/-) mice and twelve age-matched wild-type (CHL1+/+) littermates from heterozygous breeding (mixed C57BL/6J-129Ola genetic background, 5 backcrosses into C57BL/6J; Montag-Sallaz et al., 2002) were used at the age of 2 months. Genotyping of the mice from the CHL1 stock was performed using PCR assays. The animals were kept under standard laboratory conditions. All experiments were conducted in accordance with the German and European Community laws on protection of experimental animals, and the procedures used were approved by the responsible committee of The State of Hamburg. Numbers of animals studied in different experimental groups and at different time periods after surgery are given in the text and figures. All animal treatments, data acquisition and analyses were performed in a blind fashion. All technical procedures described below were performed according to Irintchev et al. (2005).

	CHL1+/+ unlesioned	CHL1+/+ lesioned	CHL1-/- unlesioned	CHL1-/- lesioned
Number	6	6	6	6

Table1: Number of animals of different genotype and health status used in this study.

3.2 Surgical procedures

For surgery, the mice were anesthetized by intraperitoneal injections of ketamin and xylazin (100 mg Ketanest®, Parke-Davis/Pfizer, Karlsruhe, Germany, and 5 mg Rompun®, Bayer, Leverkusen, Germany, per kg body weight). Laminectomy was performed at the T7-T9 level with mouse laminectomy forceps (Fine Science Tools, Heidelberg, Germany). A mouse spinal cord compression device was used to elicit compression injury (Curtis et al., 1993). Compression force (degree of closure of the forceps) and duration were controlled by an electromagnetic device. The spinal cord was maximally compressed (100%, according to the operational definition of Curtis et al., 1993) for 1 second by a time-controlled current flow through the electromagnetic device. The skin was then surgically closed using 6-0 nylon stitches (Ethicon, Norderstedt, Germany). After the operation, mice were kept in a heated room (35°C) for several hours to prevent hypothermia and thereafter singly housed in a temperature-

controlled (22°C) room with water and standard food provided *ad libitum*. During the postoperative time-period the bladders of the animals were manually voided twice daily.

3.3 Preparation of tissue for sectioning

Mice were weighed and anaesthetized with 16% solution of sodium pentobarbital (Narcoren, Merial, Hallbergmoos, 5 µl g⁻¹ body weight, i.p.). After surgical tolerance was achieved, the animals were transcardially perfused with physiologic saline for 60 seconds followed by fixative consisting of 4% formaldehyde and 0.1% $CaCl_2$ in 0.1M cacodylate buffer, pH 7.3, for 15 minutes at room temperature (RT). Following perfusion the spinal cords were left *in situ* for 2 hours at RT to reduce fixation artifacts after which they were dissected out and post-fixed overnight (18-20 hours) at 4°C in the formaldehyde solution used for perfusion. The tissue was then immersed for two days in 15% sucrose solution in 0.1M cacodylate buffer, pH 7.3, at 4°C.

Fixed and cryoprotected (sucrose-infiltrated) spinal cords were carefully examined under a stereomicroscope and rests of dura mater or other tissue debris were removed with a fine forceps. Afterwards, the lumbar spinal cords were dissected and were placed in a 1-cm-long thin foil chamber filled with Tissue Tek (Satura Finetek Europe, Zoeterwoude, The Netherlands). Finally, the spinal cords were frozen by inserting into 2-methyl-butan (isopentan) precooled to -30°C in the cryostat for 2 minutes. The spinal cords were stored in liquid nitrogen until sectioned.

3.4 Preparation of cryostat sections

For sectioning, the caudal end of each lumbar spinal cord segment was attached to a cryostat specimen holder using Tissue Tek (Satura Finetek Europe, city, country). The rostral surface of the spinal cord was oriented to face the cryostat knife edge and serial coronal sections of 25 µm thickness were cut in a cryostat Leica CM3050 (Leica Instruments, Nußloch, Germany). Sections were collected on Super Frost Plus glass slides (Roth, Karlsruhe, Germany). Since stereological analyses require extensive sectioning of the structures studied and use of spaced-serial sections (Howard and Reed, 1998), sampling was always done in a standard sequence so that 6 sections 250 µm apart were presented on each slide.

3.5 Stereological analysis of immunohistochemically defined cell types

3.5.1 Antibodies

The following commercially available antibodies were used at optimal dilutions: anti-parvalbumin (PV, mouse monoclonal, clone PARV-19, Sigma, Deisenhofen, Germany, dilllution 1:1000), anti-neuron specific nuclear antigen (NeuN, mouse monoclonal, clone A60, Sigma, 1:1000,), anti-cyclic nucleotide phophodiesterase (CNPase, mouse monoclonal, clone 11-5B, Sigma, 1:1000), anti-S-100 (rabbit polyclonal, purified IgG fraction, DakoCytomation, Hamburg, Germany, 1:500), anti-ChAT (goat polyclonal, Chemcon International, Hofheim, Germany, 1:100) and anti-Iba1 (rabbit polyclonal, affinity purified, Wako Chemicals, Neuss, Germany, 1:1500).

Antibody	Abbreviation	Type	Manufacturer	Dilution
Anti-parvalbumin	anti PV	Mouse Monoclonal, clone Parv 19	Sigma, Deisenhofen, Germany	1:1000 9.8μg/ml Ig
Anti-neuron specific nuclear antigen	Anti-NeuN	Mouse monoclonal, clone A60	Sigma	1:1000 1μg/ml Ig
Anti-cyclic nucleotide phosphatase	Anti-CNP	Mouse monoclonal, clone 11-5B	Sigma	1:1000 7.5μg/ml Ig
Anti–S-100b	Anti-S-100	Rabbit polyclonal, purified IgG fraction	DakoCytomation, Hamburg, Germany	1:500 9μg/ml Ig
Anti-choline acetyltransferase	Anti-ChAT	Goat polyclonal	Chemcon International, Hofheim, Germany	1:100 1μg/ml Ig
Anti-Iba1	Anti-Iba1	Rabbit polyclonal, affinity purified	Wako Chemicals, Neuss, Germany	1:1500 0.3μg/ml Ig

Table 2: Commercial antibodies used in this study.

The antibodies used in this study recognize specific cell-marker antigens known to be expressed in defined cell populations in the spinal cord (Irintchev et al., 2005):

NeuN (neuron-specific nuclear antigen) is a protein of unknown function shown to be present in all neurons in the adult CNS with the exception of a few cell types (Purkinje, mitral and photoreceptor cells, Wolf et al., 1996).

PV (parvalbumin) is a low molecular weight calcium-binding protein expressed in a major subpopulation of GABAergic neurons in the CNS (Celio, 1986).

S-100b is a low molecular weight calcium-binding protein expressed in astrocytes.

CNPase (2´,3´-cyclic nucleotide 3´-phosphodiesterase) is an enzyme present only in cells which are able to synthesize myelin, i.e. oligodendrocytes and Schwann cells.

Iba1 is a macrophage/microglia-specific calcium-binding protein involved in the activation of quiescent microglial cells (Imai and Kohsaka, 2002).

ChAT (choline acetyltransferase) is an enzyme which marks cholinergic neurons including motoneurons.

3.5.2 Immunohistochemical stainings

Immunohistochemical stainings were performed as described (Irintchev et al., 2005). The immunohistochemistry was done on 25 μm thick sections. Sections, stored at -20°C, were air-dried for 30 minutes at 37°C. A 10 mM sodium citrate solution (pH 9.0, adjusted with 0.1 M NaOH) was prepared and pre-heated in a jar to 80°C in a water bath. The sections were incubated at 80°C for 30 minutes and afterwards the jar was taken out and left to cool down at room temperature. Afterwards, blocking of unspecific binding sites was performed. The sections were incubated at room temperature for one hour in PBS containing 0.2% Triton X-100 (Fluka, Buchs, Germany), 0.02% sodium azide (Merck, Darmstadt, Germany) and 5% normal goat or donkey serum (Jackson Immuno Research Laboratories, Dianova, Hamburg, Germany). The selection of normal serum for blocking was determined by the species in which the secondary antibody was produced (see below). After one hour the blocking solution was aspired and the slices were incubated with the primary antibody diluted in PBS containing 0.5% lambda-carrageenan and 0.02% w/v sodium azide in PBS. The slides were incubated for 3 days at 4°C in a screw-cap staining jar (30 ml capacity, Roth). Following this, the sections were washed 3 times in PBS (15 minutes each) before an appropriate (anti-rabbit, anti-mouse or anti-goat) secondary antibody was applied. The sections were incubated with the second antibody diluted (1:200) in PBS-carrageenan at RT for 2 hours. Goat anti-rabbit, goat anti-mouse and donkey anti-goat IgG conjugated with Cy3 (Jackson Immuno Research Laboratories, Dianova, Hamburg, Germany) were used. After a subsequent wash in PBS, cell nuclei were stained for 10 minutes at RT with bis-benzamine solution (Hoechst 33258 dye, 5 μg/ml in PBS, Sigma). Finally, the sections

were washed again, mounted with Fluoromount G (Southern Biotechnology Associates, Biozol, Eching, Germany) and stored in the dark at 4°C.

3.5.3 Stereological analyses

The optical dissector method was chosen for quantitative analysis because of its efficiency, an important prerequisite when aiming to quantify numerical densities of a variety of cell types in a given CNS region (Irintchev et al., 2005). The method consists of direct counting of objects in relatively thick sections (e.g., 25 – 50 μm) under the microscope using a three-dimensional counting frame ("counting brick", see Howard and Reed 1998, referred to here simply as dissector) to "probe" the tissue at random. The base of the frame (dimensions in the x/y plane) is defined by the size of the squares formed by a grid projected into the visual field of the microscope. The height of the dissector is a portion of the section thickness defined by two focus planes in the z axis at a distance of x μm. Control of this parameter is achieved by use of mechanic or electronic devices measuring the movement of the microscope stage in the z axis. Objects (e.g., cells) within each dissector are counted according to stereological rules: Those entirely within the dissector as well as those touching or being dissected by the "acceptance", but not the "forbidden" planes of the frame are counted (Howard and Reed, 1998).

The cell counts were performed on an Axioskope microscope (Zeiss, Oberkochen, Germany) equipped with a motorized stage and Neurolucida software-controlled computer system (MicroBrightField, Colchester, USA). Sections were observed under low-power magnification (10x objective) with a 365/420 nm excitation/emission filter set (01, Zeiss, blue fluorescence). The nuclear staining allows delineation of spinal cord structures and areas.

The viewed area was randomized by setting a reference point at an arbitrary place resulting in an overlay of the visible field by a gird with lines spaced 30 μm (NeuN and Iba1) or 60 μm (S-100 and CNPase). The contours of the area of interest were outlined with the cursor. Squares within the marked area at distances of 60 μm (Iba1, PV, NeuN) or 120 μm (S-100, CNPase) apart for the other squares were labeled with a symbol starting from the uppermost left side of the delineated field. A dissector depth of 10 μm was chosen since antibody penetration was sufficient to enable clear recognition of stained objects within a depth of at least 10 μm. The sections were then viewed with the 40x objective and 546/590nm excitation/emission filter set 15, Zeiss, red fluorescence.

The marked meander was scanned and all marked frames were viewed consecutively. Immunolabeled cell profiles that were entirely within the counting frame at any focus level, as well as those attaching to or crossing by the acceptance planes were marked with a symbol. Then, by repeated switching between red and blue filter sets and changing the focus plane, the nuclei of the labeled cells were identified. All nuclei that were in focus beyond a guard space (depth 0-2 μm from the section surface), i.e. lying within 2 and 12 μm below the top of the section, were counted except those at the "look-up" level (2 μm) and such crossing or touching the forbidden planes. Six sections spaced 250 μm apart were evaluated bilaterally per animal and staining. For PV- and ChAT-positive neurons, no gird used; all positive neurons in the ventral (ChAT, PV) and dorsal horn (PV) with nuclei within the depth of disector were counted.

3.5.4 Estimation of volume of the spinal cord

The volume of a defined segment of the lumbar spinal cord (1.5 mm length) was estimated according to the method of Cavalieri (Howard and Reed, 1998). The entire spinal cord, the ventral and dorsal gray matter and the white matter were outlined and their areas, estimated by the computer, were used to calculate volumes (in mm^3) by multiplying the sum of the areas per section (left and right side averaged for each section) by the distance between sections, i.e. 250 μm. Total number of cells were calculated by multiplying cell density by volume of the reference space.

3.5.5 Photographic documentation

Photographic documentation was made on a confocal microscope (FV10-ASW, Olympus, Hamburg, Germany).

3.5.6 Statistical analysis

Mean values were compared using the two-sided t test for independent groups. By two or more measurements per parameter and animal, the mean was used as a representative value. Thus, for all comparisons the degree of freedom was determined by the number of animals. The accepted level of significance was 5%.

3.5.7. Immunohistochemical markers and quality of staining

For each particular antigen, all sections were stained in the same primary and secondary antibody solutions kept in staining jars and stabilized in order to enable repeated long-term usage (Sofroniew and Schrell, 1982; Irintchev et al., 2005). The previously documented reproducibility of this staining technique was also apparent in this study: the quality of staining remained constant for all batches of slides processed over a period of several months, an important prerequisite for quantitative studies on a large number of animals. No qualitative differences between CHL1+/+ and CHL1-/- animals were noticed in the staining patterns for the detected antigens. Examples of the stainings are shown in Figure 1 and Figure 2.
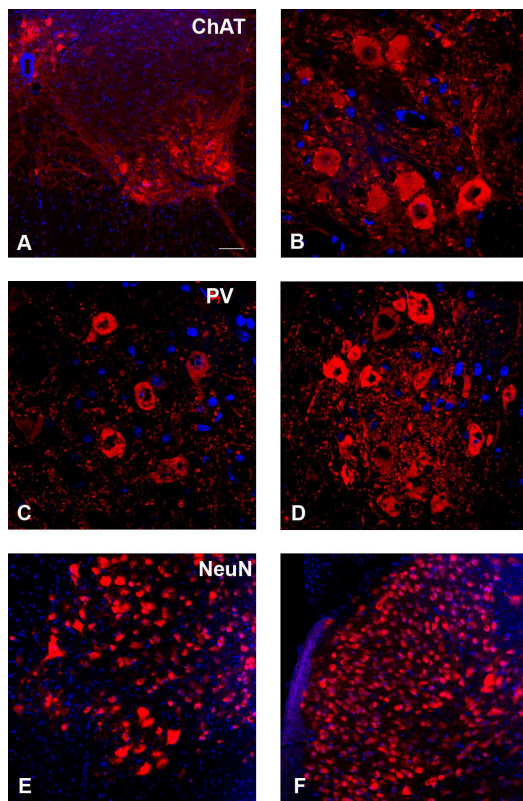

Figure 1: Representative images of ChAT (A,B), PV (C,D) and NeuN (E,F) stainings (red) with nuclear counterstaining (blue) in the ventral (C,E) and dorsal (D,F) horns of uninjured spinal cords. Scale bar: 60μm (A), 20μm (B-D), 40μm (E,F).
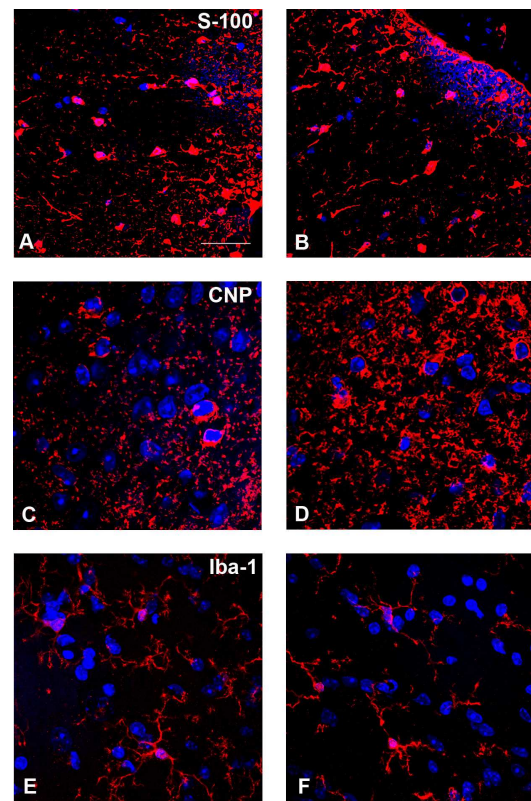
Figure 2: Representative images of S-100 (A,B), CNP (C,D) and Iba1 (E,F) stainings (red) with nuclear counterstaining (blue) in the gray (A,C,E) and the white (B,D,F) matter of uninjured spinal cords. Scale bar: 60μm.

4 RESULTS

4.1. Neuronal and glia cell populations in intact and spinal cord-injured CHL1+/+ (C57BL/6) mice

4.1.1 Total number of cells

The total number of cells was estimated by using the nuclear staining. No significant difference in the overall cell number was found between the intact and injured animals in the lumbar spinal cord (Figure 3).
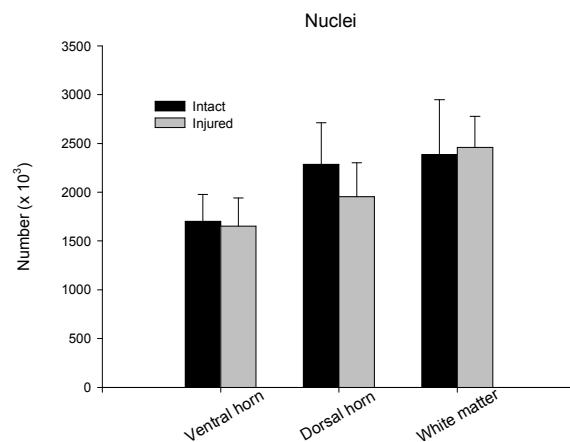

Figure 3: Number of cell nuclei in the lumbar spinal cord of intact (black bars) and injured animals (grey bars) in the ventral horn (left bar pair), dorsal horn (middle bar pair) and white matter (right bar pair). Shown are mean values + SD. No significant differences between the groups were found (two-sided t test for independent samples, $p < 0.05$).

4.1.2 Neurons

The estimation of the numbers of NeuN-positive neurons showed a significant difference between injured and intact animals. A reduction in the number of neurons after injury could be seen in the ventral horn (-24%) as well as in the dorsal horn (-10%, Figure 4), but only the reduction in the ventral horn was statistically significant. NeuN-positive neurons were not detected in the white matter either before or after injury.
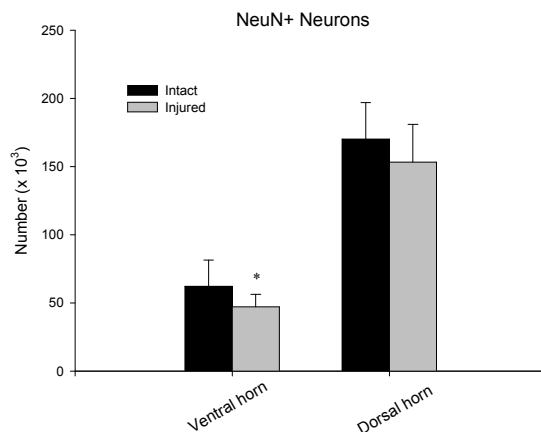

Figure 4: Number of NeuN-positive neurons in the lumbar spinal cord of intact (black bars) and injured animals (grey bars) in the ventral horn (left bar pair) and dorsal horn (right bar pair). Shown are mean values + SD. The asterisk indicates a significant difference as compared to the intact group (two-sided t test for independent samples, $p < 0.05$).

4.1.3 Motoneurons

A large and statistically significant decline was revealed in the number of ChAT-positive motoneurons in ventral horns of injured animals compared with intact controls (-35%, Figure 5).
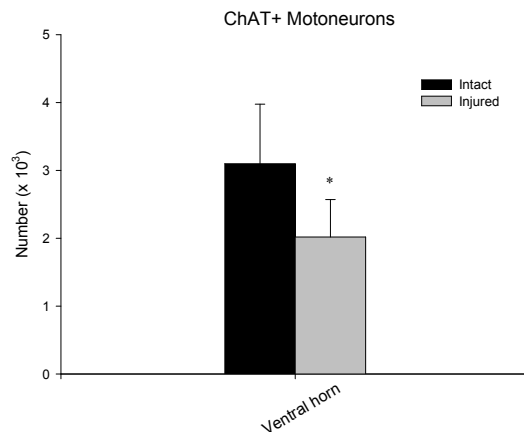

Figure 5: Number of ChAT-positive motoneurons in the lumbar spinal cord of intact (black bars) and injured animals (grey bars) in the ventral horn. Shown are mean values + SD. The asterisk indicates a significant difference as compared to the intact group (two-sided *t* test for independent groups, p < 0.05).

4.1.4 PV-positive interneurons

After injury there is a large and statistically significant loss of PV-positive GABAergic neurons in the entire grey matter of the lumbar spinal cord. In the ventral horn a loss of over 40% PV-expressing cells was detected after injury (Figure 6). The results for the dorsal horn were similar: injured animals had approximately 50% fewer PV-positive interneurons than the intact control group (Figure 6).
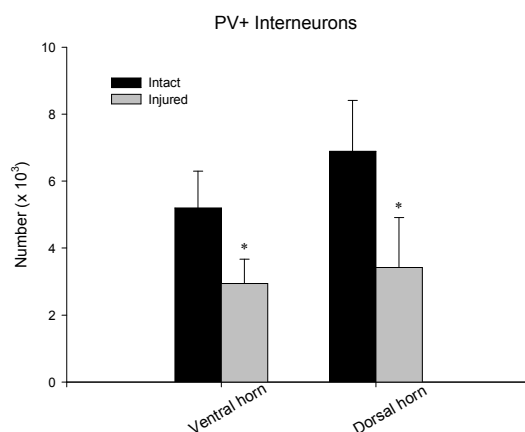

Figure 6: Number of PV-positive neurons in the lumbar spinal cord of intact (black bars) and injured animals (grey bars) in the ventral horn (left bar pair) and the dorsal horn (right bar pair). Shown are mean values + SD. The asterisks indicate significant differences as compared to the intact group (two-sided *t* test for independent groups, p < 0.05).

4.1.5 Astrocytes

No significant differences were detected between the numbers of S-100-positive astrocytes in the gray matter of injured animals compared with intact ones (Figure 7). Since in the white matter we could not detect any S-100 staining associated with the cell nuclei, astrocytes in this region were not counted.
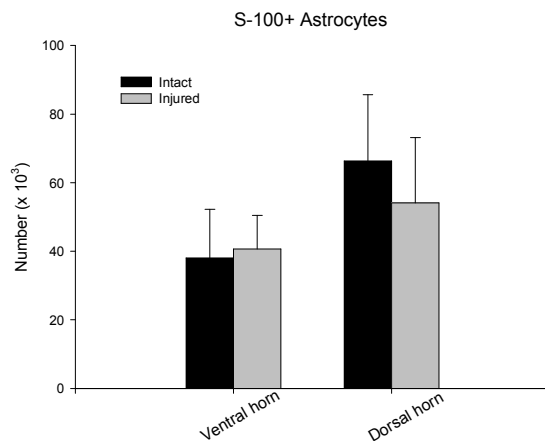

Figure 7: Number of astrocytes in the lumbar spinal cord of intact (black bars) and injured animals (grey bars) in ventral horn (left bar pair) and dorsal horn (right bar pair). Shown are mean values + SD. No significant differences between the groups were found (*t* test).

4.1.6 Oligodendrocytes

Comparing the intact and injured animals there were no significant differences in number of CNP-positive oligodendrocytes in the grey matter. However, a relatively large cell loss of around 32% was detected in the white matter (Figure 8).
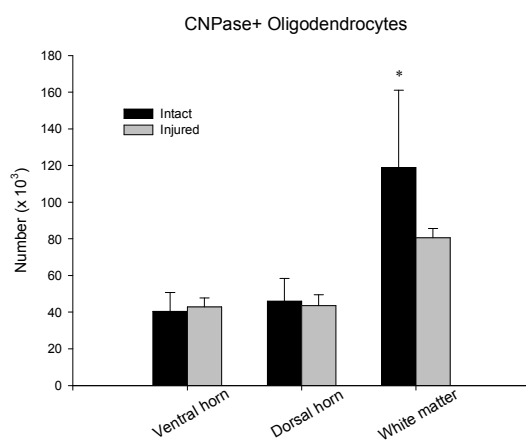

Figure 8: Number of oligodendrocytes in the lumbar spinal cord of intact (black bars) and injured animals (grey bars) in the ventral horn (left bar pair), the dorsal horn (middle bar pair) and the white matter (right bar pair). Shown are mean values + SD. The asterisk indicates a significant difference as compared to the intact group (two-sided *t* test for independent groups, $p < 0.05$).

4.1.7 Microglial cells

Iba1, a recently discovered calcium-binding protein, is involved in the activation of microglia and thus expressed in quiescent cells (Imai and Kohsaka, 2002). Following activation, the protein expression is enhanced and maintained at high levels in activated microglia. This allows reliable identification of both resting and activated microglial cells.

After injury, an increase of about 90% compared with intact mice was detected in the number of microglial cells in the ventral horn (Figure 9). Mean numbers of Iba1-positive cells were also higher, by about 30% compared with intact mice, in the dorsal horn and the white matter but the differences between intact and injured groups were not statistically significant.

A characteristic feature of the injured spinal cord was that microglial cells often appeared in clusters (Figure 26). Such clusters were not seen in the white matter of intact spinal cords.
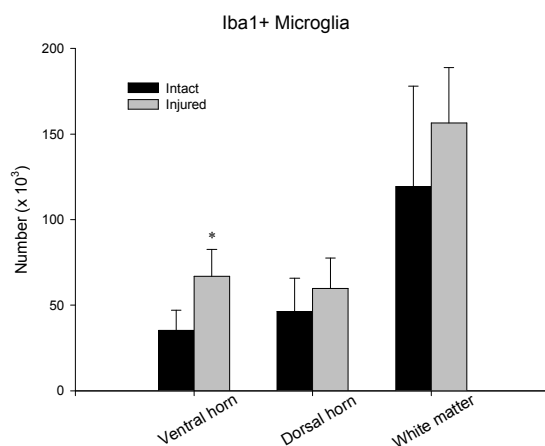

Figure 9: Number of microglial cells in the lumbar spinal cord of intact (black bars) and injured animals (grey bars) in the ventral horn (left bar pair), dorsal horn (middle bar pair) and the white matter (right bar pair). Shown are mean values + SD. The asterisk indicates a significant difference as compared to the intact group (two-sided *t* test for independent groups, $p < 0.05$).

4.1.8 Summary of changes in cell populations after spinal cord injury in CHL1+/+ (C57BL/6) mice

Cell type	Region	Change
Nuclei	VH	=
	DH	=
	WM	=
NeuN$^+$ neurons	VH	↓ (-24 %)
	DH	=
ChaT$^+$ motoneurons	VH	↓ (-35%)
PV$^+$ neurons	VH	↓ (-40%)
	DH	↓ (-50%)
S-100$^+$ astrocytes	VH	=
	DH	=
CNP$^+$ oligodendrocytes	VH	=
	DH	=
	WM	↓ (-32%)
Iba1$^+$ microglia	VH	↑ (+90%)
	DH	= (+30%)
	WM	= (+32%)

Table 3: Summary of changes in cell populations in the lumbar spinal cord after injury.

4.2 Cell populations before and after injury in CHL1-/- vs. CHL1+/+ mice

4.2.1 Total numbers of cells

Comparing the total cell number of CHL-/- animals with the number in the wild-type control group showed no significant differences between the genotypes before and after injury (Figures 10-12).
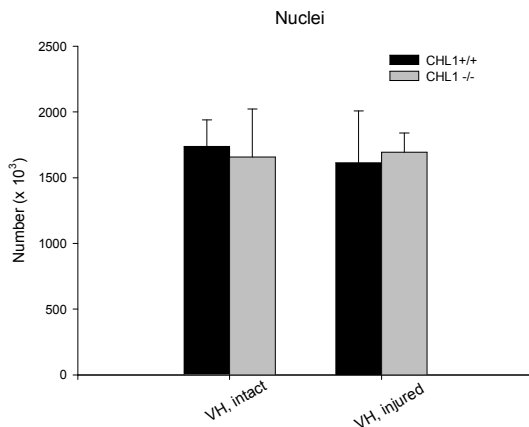

Figure 10: Total number of cell nuclei in the lumbar spinal cord of CHL1+/+ (black bars) and CHL1-/- animals (grey bars) in intact (left bar pair) and injured mice (right bar pair) in the ventral horn. Shown are mean values + SD. No significant differences between the groups were found (*t* test).

Figure 11: Total number of cell nuclei in the lumbar spinal cord of CHL1+/+ (black bars) and CHL1-/- animals (grey bars) in intact (left bar pair) and injured mice (right bar pair) in the dorsal horn. Shown are mean values + SD. No significant differences between the groups were found (*t* test).
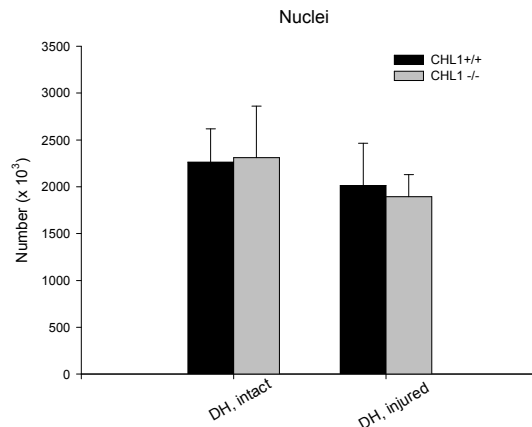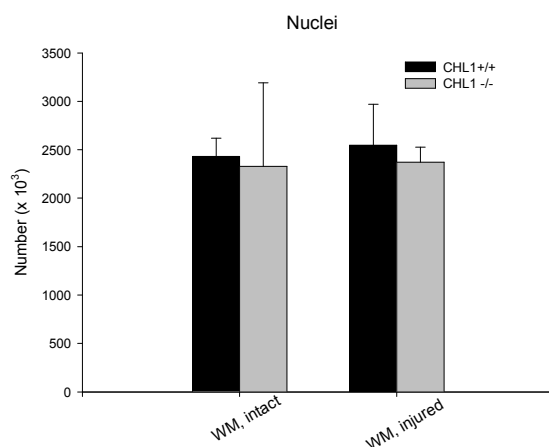

Figure 12: Total number of cell nuclei in the lumbar spinal cord of CHL1+/+ (black bars) and CHL1-/- animals (grey bars) in intact (left bar pair) and injured mice (right bar pair) in the white matter. Shown are mean values + SD. No significant differences between the groups were found (*t* test).

4.2.2 Neurons

No significant differences between CHL1-/- and CHL1+/+ mice were found in the ventral horn before and after injury (Figure 13), but the number of NeuN-positive neurons was by 25% higher in the dorsal horn of CHL1-/- than CHL1+/+ mice before injury (Figure 14).
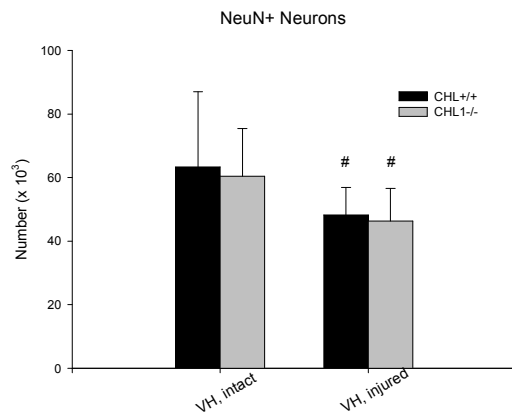

Figure 13: Number of Neu-N-positive neurons in the lumbar spinal cord of CHL1+/+ (black bars) and CHL1-/- animals (grey bars) in intact (left bar pair) and injured mice (right bar pair) in the ventral horn. Shown are mean values + SD. Crosshatches indicate significant differences as compared to the intact group (two-sided *t* test for independent groups, p < 0.05).
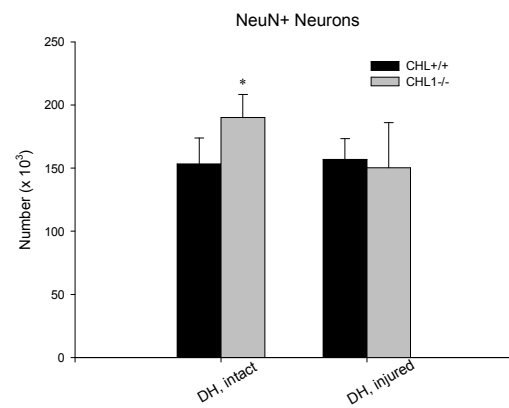
Figure 14: Number of Neu-N-positive neurons in the lumbar spinal cord of CHL1+/+ (black bars) and CHL1-/- animals (grey bars) in intact (left bar pair) and injured mice (right bar pair) in the dorsal horn. Shown are mean values + SD. The asterisk indicates a significant difference as compared to the wild-type group (two-sided *t* test for independent groups, p < 0.05).

4.2.3 Motoneurons

The loss of ChAT-positive motoneurons after injury was present in both CHL1+/+ and CHL1-/- mice. Both before and after injury numbers of motoneurons in the lumbar spinal cords were similar in CHL1-/- mice and their wild-type littermates (Figure 15).

Figure 15: Number of ChAT-positive motoneurons in the lumbar spinal cord of CHL1+/+ (black bars) and CHL1-/- animals (grey bars) in intact (left bar pair) and injured mice (right bar pair). Shown are mean values + SD. Crosshatches indicate significant differences as compared to the intact group (two-sided t test for independent groups, p < 0.05).
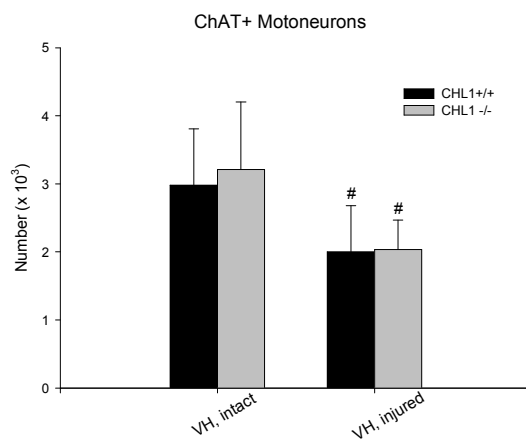
4.2.4 PV-positive interneurons

Numbers of PV-positive neurons were similar in CHL1-/- and CHL1+/+ mice before injury in the ventral horn (Figure 16). SCI caused reduction of PV-positive neuron numbers in both genotypes. This reduction was more pronounced in CHL1-/- than in CHL1+/+ mice leading to a significant deficit (-29%) in injured CHL1-/- mice compared with injured CHL1+/+ littermates (Figure 16). No differences between the genotypes were found in the dorsal horn (Figure 17).

Figure 16: Number of PV-positive neurons in the lumbar spinal cord of CHL1+/+ (black bars) and CHL1-/- animals (grey bars) in intact (left bar pair) and injured mice (right bar pair) in the ventral horn. Shown are mean values + SD. The asterisk indicates a significant difference as compared to the wild-type group. Crosshatches indicate significant differences as compared to the intact group (two-sided t test for independent groups, p < 0.05).
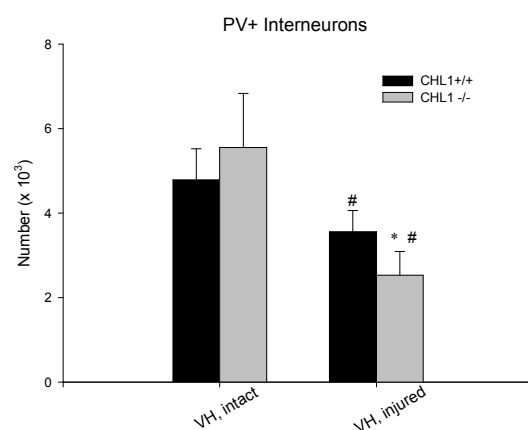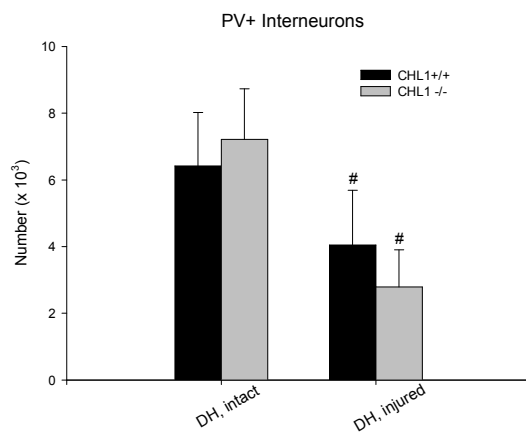
Figure 17: Number of PV-positive neurons in the lumbar spinal cord of CHL1+/+ (black bars) and CHL1-/- animals (grey bars) in intact (left bar pair) and injured mice (right bar pair) in the dorsal horn. Shown are mean values + SD. Crosshatches indicate significant differences as compared to the intact group (two-sided *t* test for independent groups, p < 0.05).

4.2.5 Astrocytes

In the ventral horn, as well as in the dorsal horn, there were no significant differences between the genotypes before and after injury (Figure 18, Figure 19).

Figure 18: Number of astrocytes in the lumbar spinal cord of CHL1+/+ (black bars) and CHL1-/- animals (grey bars) in intact (left bar pair) and injured mice (right bar pair) in the ventral horn. Shown are mean values + SD. No significant differences between the groups were found (*t* test).

Figure19: Number of astrocytes in the lumbar spinal cord of CHL1+/+ (black bars) and CHL1-/- animals (grey bars) in intact (left bar pair) and injured mice (right bar pair) in the dorsal horn. Shown are mean values + SD. No significant differences between the groups were found (*t* test).

4.2.6 Oligodendrocytes

No significant differences between the genotypes were found for CNPase-positive oligodendrocytes in the ventral horn, dorsal horn and the white matter before and after injury (Figures 20-22).

Figure 20: Number of oligodendrocytes in the lumbar spinal cord of CHL1+/+ (black bars) and CHL1-/- animals (grey bars) in intact (left bar pair) and injured mice (right bar pair) in the ventral horn. Shown are mean values + SD. No significant differences between the groups were found (*t* test).
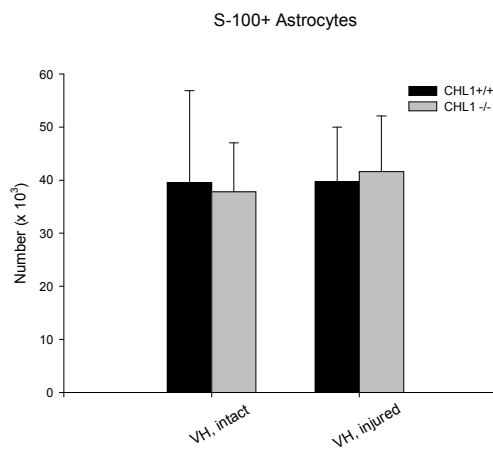

Figure 21: Number of oligodendrocytes in the lumbar spinal cord of CHL1+/+ (black bars) and CHL1-/- animals (grey bars) in intact (left bar pair) and injured mice (right bar pair) in the dorsal horn. Shown are mean values + SD. No significant differences between the groups were found (*t* test).
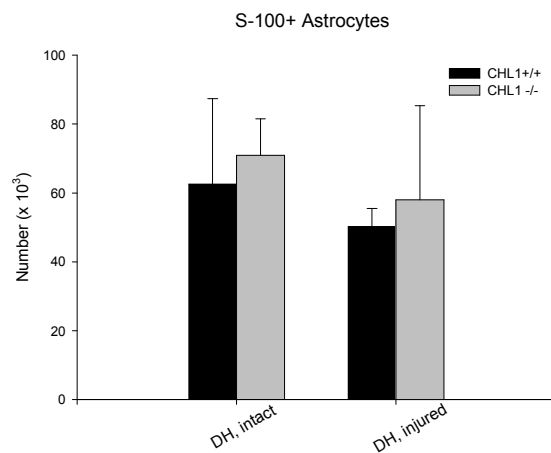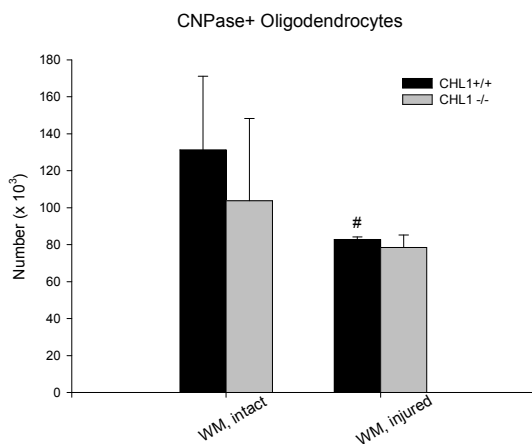

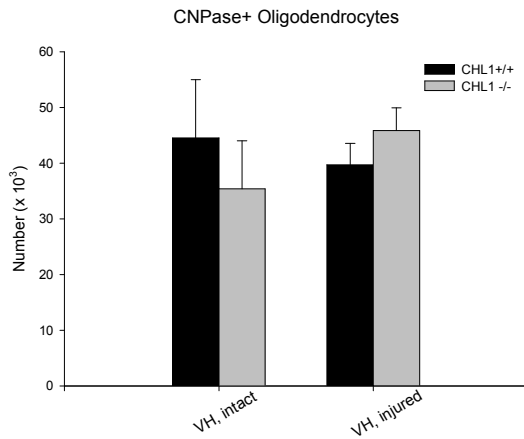**Figure 22:** Number of oligodendrocytes in the lumbar spinal cord of CHL1+/+ (black bars) and CHL1-/- animals (grey bars) in intact (left bar pair) and injured mice (right bar pair) in the white matter. Shown are mean values + SD. The crosshatch indicates a significant difference as compared to the intact group (two-sided *t* test for independent groups, $p < 0.05$).

4.2.7 Microglial cells

In the ventral horn of the injured lumbar spinal cords, a higher number of microglial cells was detected in CHL1-/- mice than in their wild-type littermates (Figure 23). There were no differences between the genotypes in the dorsal horn and white matter (Figure 24, Figure 25).
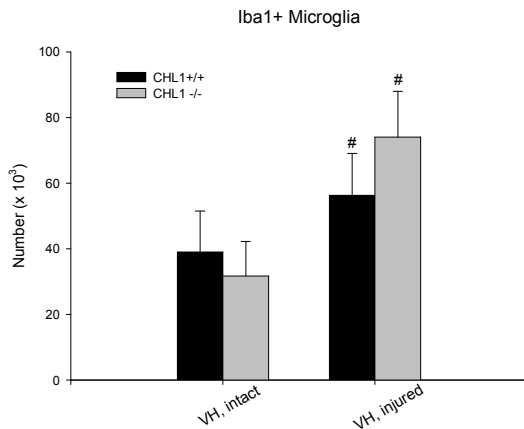
Figure 23: Number of microglial cells in the lumbar spinal cord of CHL1+/+ (black bars) and CHL1-/- animals (grey bars) in intact (left bar pair) and injured mice (right bar pair) in the ventral horn. Shown are mean values + SD. Crosshatches indicate significant differences as compared to the intact group (two-sided *t* test for independent groups, p < 0.05).
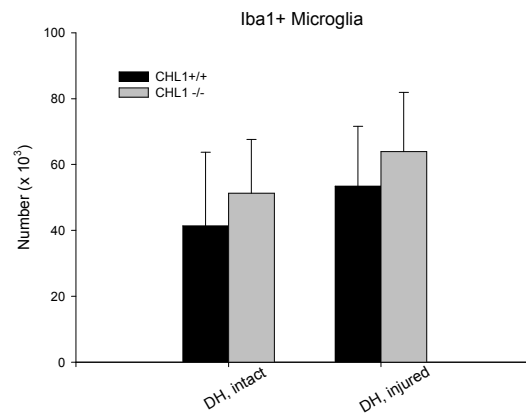
Figure 24: Number of microglial cells in the lumbar spinal cord of CHL1+/+ (black bars) and CHL1-/- animals (grey bars) in intact (left bar pair) and injured mice (right bar pair) in the dorsal horn. Shown are mean values + SD. No significant differences between the groups were found (*t* test).
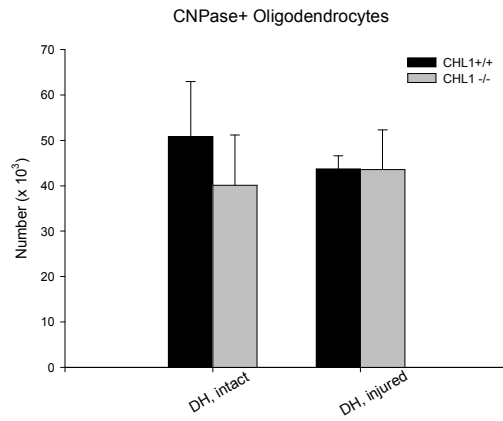

Figure 25: Number of microglial cells in the lumbar spinal cord of CHL1+/+ (black bars) and CHL1-/- animals (grey bars) in intact (left bar pair) and injured mice (right bar pair) in the white matter. Shown are mean values + SD. No significant differences between the groups were found (*t* test).

In both wild-type and CHL1-/- mice, microglial clusters were detected in the white matter of injured spinal cords (Figure 27). Their number was similar in the two genotypes (Figure 26). Such clusters were not observed in the intact spinal cord of CHL1-/- and CHL1+/+ mice.
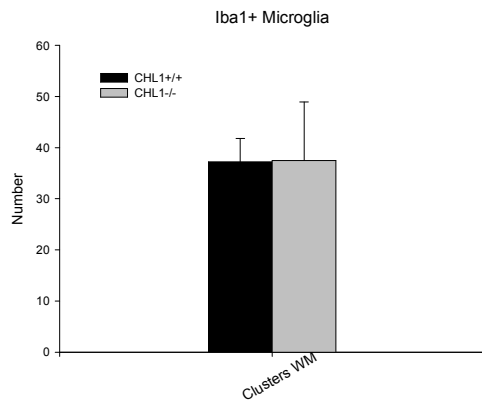
Figure 26: Number of microglia clusters per cross-section from the lumbar spinal cord of CHL1+/+ (black bar) and CHL1-/- animals (grey bar) in injured mice in the white matter. Shown are mean values + SD. No significant differences between the groups were found (*t* test).

The morphology of microglial cells changes after injury (reactive microglia): the size of the cell body is enlarged and the slender cell processes become thicker, shorter and can even disappear completely in phagocytic microglia (Streit et al., 1999). While resting microglial cells are evenly distributed throughout the tissue as single cells, activated cells form aggregates in areas of cell death. Both signs of activation of single Iba1-positive cells and clusters were seen in CHL1-/- as well as in CHL+/+ animals after injury.
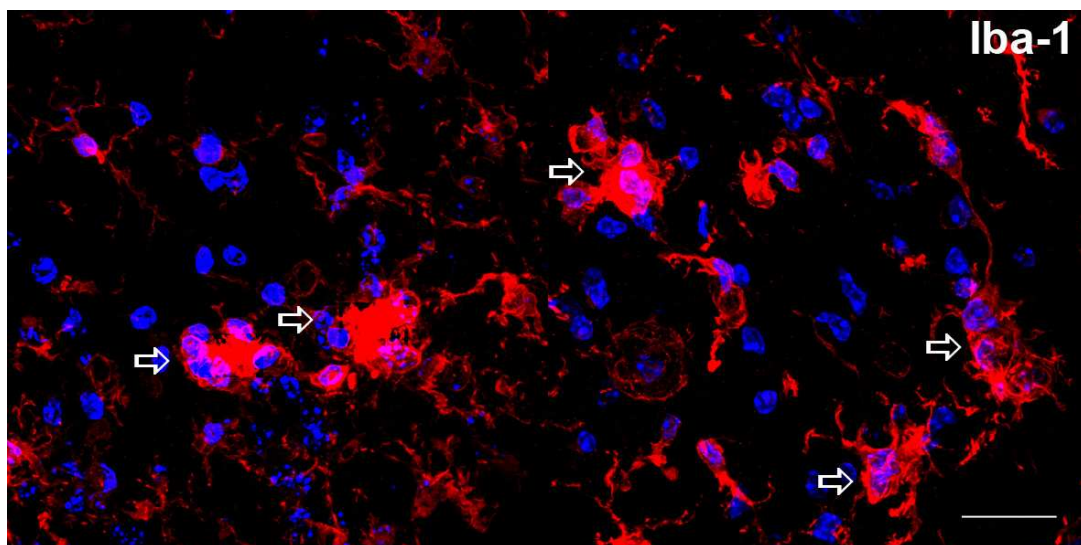
Figure 27: Representative image showing Iba1^{+} clusters of microglial cells (arrows) in the white matter of an injured spinal cord. Scale bar: 50μm.

4.3 Morphometric analysis of the spinal cord

4.3.1 Volume of the lumbar spinal cord after spinal cord injury in CHL1+/+ (C57BL/6) mice

In comparison to intact animals, the volume of the spinal cords of injured wild-type mice was strongly reduced (Figure 28). The degree of reduction was similar among the three areas studied, ventral horn, dorsal horn and white matter (32-34%).
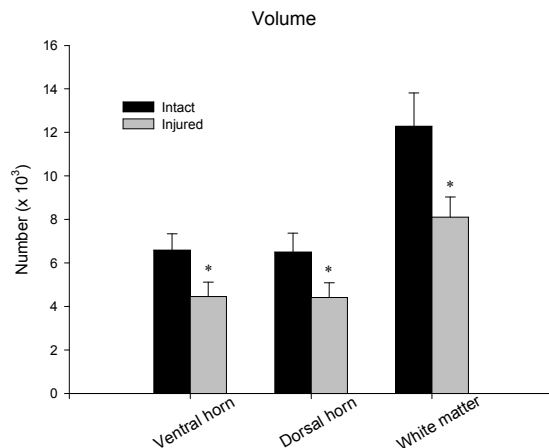
Figure 28: Volume of the lumbar spinal cord of intact (black bars) and injured wild-type mice (grey bars) in the ventral horn (left bar pair), the dorsal horn (middle bar pair) and the white matter (right bar pair). Shown are mean values + SD. Asterisks indicate significant differences as compared to the intact group (two-sided *t* test for independent groups, p < 0.05).

4.3.2 Volume of the lumbar spinal cord before and after injury in CHL1-/- vs. CHL1+/+ mice

The volumes of the ventral horn, dorsal horn and white matter were similar in uninjured CHL1-/- and CHL1+/+ mice (Figures 29-31). The degree of spinal cord volume reduction after injury was similar in the two genotypes (Figures 29-31).

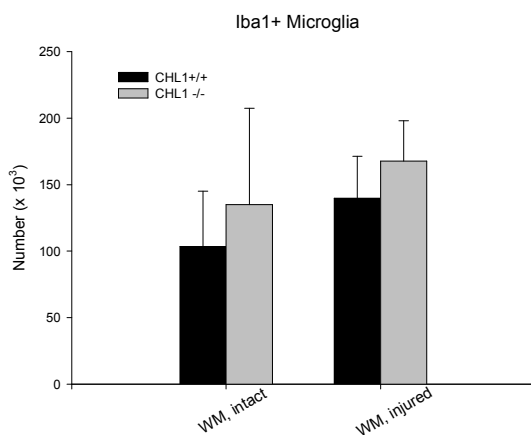**Figure 29:** Volume of the lumbar spinal cord of CHL1+/+ (black bars) and CHL1-/- animals (grey bars) in intact (left bar pair) and injured mice (right bar pair) in the ventral horn. Shown are mean values + SD. Crosshatches indicate significant differences as compared to the intact group (two-sided *t* test for independent groups, p < 0.05).
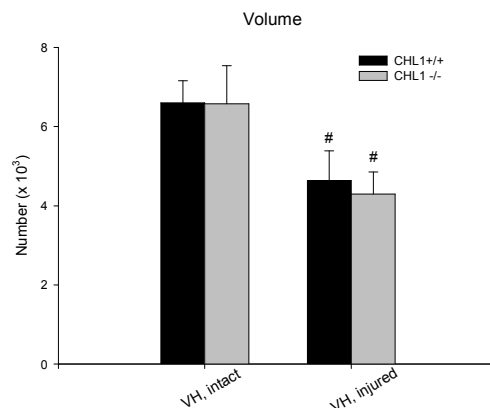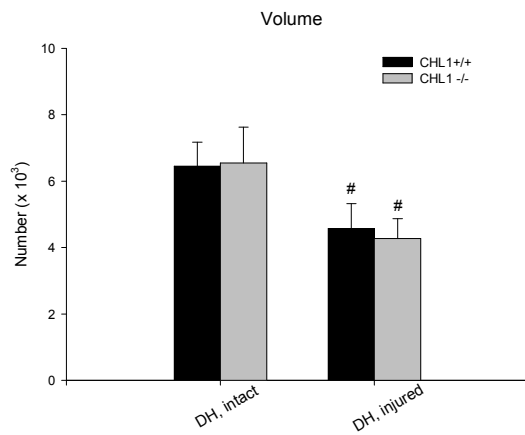
Figure 30: Volume of the lumbar spinal cord of CHL1+/+ (black bars) and CHL1-/- animals (grey bars) in intact (left bar pair) and injured mice (right bar pair) in the dorsal horn. Shown are mean values + SD. Crosshatches indicate significant differences as compared to the intact group (two-sided t test for independent groups, $p < 0.05$).
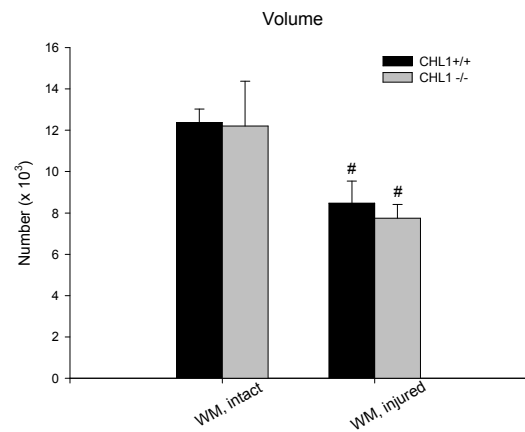
Figure 31: Volume of the lumbar spinal cord of CHL1+/+ (black bars) and CHL1-/- animals (grey bars) in intact (left bar pair) and injured mice (right bar pair) in the white matter. Shown are mean values + SD. Crosshatches indicate significant differences as compared to the intact group (two-sided t test for independent groups, $p < 0.05$).

4.3.3 Summary of changes in the volume of spinal cord columns and in the total number of cells after injury in wild-type mice

Type	Region	Change
Volume	VH	↓ (-32%)
	DH	↓ (-32%)
	WM	↓ (-34%)
Nuclei	VH	=
	DH	=
	WM	=

Table 4: Summary of changes in volume and total cell number in the lumbar spinal cord after injury in wild-type mice. Similar results were obtained for CHL1-/- mice.

5 DISCUSSION

The main aim of this work was to investigate the changes in the cellular composition of the lumbar spinal cord in the chronic phase after severe lower thoracic compression injury. The most striking finding was, as of yet unrecognized, but intuitively expected shrinkage of the lumbar spinal cords upon lower thoracic compression. This loss of volume is expectable, since axonal degeneration and consequent demyelination are prominent features of SCI pathology. Furthermore, as discussed below, all major cellular populations in the spinal cord, with the exception of microglia, are either decreased or unchanged after injury (Table 3). In the mouse spinal cord complete transection model, Bjugn and colleagues (1997) have observed a loss of approximately 20% of the ventral horn volume upon injury, but no changes in the number of ventral horn neurons. These authors explained this loss of volume mostly by a reduction in the size of the neuropil (Bjugn et al., 1997). The presented observations suggest a larger (>30%) loss of volume both in the gray matter (ventral and dorsal horn) and in the white matter.

5.1 Neuronal loss after spinal cord injury

5.1.1 Motoneurons

Injury to the spinal cord causes massive tissue destruction and total neuronal loss at the site of injury. Since connections between higher centers and lumbar spinal cord are disrupted, considerable deafferentation affects spinal neurons, including motoneurons. It has long been hypothesized that this deafferentation leads to anterograde transsynaptic degeneration of neurons, especially motoneurons after SCI, but the evidence has been conflicting (Young, 1966; Bjugn et al., 1997).

Anterograde transsynaptic degeneration after injury is caused by afferent denervation of neurons remote from the site of injury and is reported in various CNS injury paradigms (Cowan, 1970). In the spinal cord, loss of sensory input after peripheral nerve injury induces degeneration of spinal cord projection and/or interneurons in the dorsal horns (Knyihar Csillil et al., 1989; Hama et al., 1996). During development, the loss of dorsal root afferents also affects motoneurons and spinal cord transection causes a significant loss of motoneurons distal to the lesion site (Young, 1966; Okado and Oppenheim, 1984). Data about loss of motoneurons after SCI in adult mammals are, however, conflicting. Some investigators have detected a substantial

reduction in the number of ventral horn neurons (Young, 1966; Eidelberg et al., 1989; Dong Teng et al., 1999), whereas other have found no change in motoneuronal numbers (McBride and Feringa, 1992; Bjugn et al., 1997). There are, however, significant differences among these studies, and between those and our study, with regard to the species, injury severity and methods of counting. Both Young (1966) and Eidelberg and colleagues (1989) studied the effect of a complete lower thoracic spinal cord transection in adult cats and rats, respectively, and they both detected loss in numbers of motoneruons in L7 and L4-5 segments, respectively. Especially interesting is the study of Eidelberg et al. (1989) on rats, which showed a decline in the number of motoneurons after complete thoracic transection in the lumbar, but not in the cervical spinal cord, and no change in lumbar motoneuron number after complete ablation of the cerebellum or motor cortex. These authors attributed motoneuronal loss to destruction of descending spinal axons, and also demonstrated that treatment with GABA agonists or calcium channel blocker did not prevent motoneuronal loss (Eidelberg et al, 1989). An attempt to reproduce this study failed to demonstrate loss of retrogradely labelled sciatic nerve motoneurons at 10, 20 and 52 weeks after complete transection of rat thoracic spinal cords (McBride and Feringa, 1992). However, since these authors used retrograde tracing of motoneurons, procedure that can by itself cause neuronal damage and degeneration, and counted only traced motoneurons, their evidence is not conclusive. Another more recent study using stereological techniques reported no loss of ventral horn neurons in the lumbar spinal cord after transection of the rat spinal cord, but those authors counted Nissl-stained neurons in the ventral horn indiscriminately (Bjugn et al., 1997). Since motoneurons comprise only a proportion of all ventral horns neurons (according to our estimate around 6%), it is possible that a moderate loss of motoneuron population was missed (Bjugn et al., 1997). These authors, however, rise several interesting points regarding motoneuronal loss after SCI. Firstly, inter-species differences have to be taken into account, especially since in primates (including humans) corticospinal neurons project more abundantly to the ventral horns and motoneurons, whereas in rodents they mostly synapse in the intermediate grey matter and dorsal horn (Bjugn et al., 1997). Second important problem is the decrease in motoneuron soma size after injury. Neuronal degeneration and death is usually accompanied by shrinkage of cell bodies and dendrites. The lack of consensus between studies on this important question suggests that there is a genuine difference in the trophics of motoneurons among various injury paradigms.

The most important question that remains unresolved by our study is whether the decrease in number of ChAT$^+$ motoneurons was due to actual cell death and loss of motoneurons, or due to down-regulation of ChAT expression in their cell bodies? One way to address this question would be to count Nissl-stained sections and identify motoneurons by their size and position (Young, 1966; Bjugn et al., 1997). However, this method of motoneuron detection is not completely reliable even if performed by a very experienced examiner. Another way would be to search for morphological evidence for motoneuron death at different time-points after injury. It would be interesting to determine, at ultramicroscopic level, if there are signs of motoneuronal degeneration in our model similar to these described after complete spinal cord transection in rats (Eidelberg et al., 1989).

Finally, there is evidence that functional recovery after SCI is not dependent on the preservation of motoneurons. Dong Teng et al. (1999), for example, treated injured rat spinal cords with basic fibroblast growth factor (FGF2), and reported improved survival of motoneurons, and better respiratory function in FGF2 treated animals 5 weeks after spinal cord contusion. No effects of FGF2 on locomotor function, however, were reported in this study. Electrophysiological studies of motor units in cats have demonstrated that motor units caudal to injury are functioning normally after transection (Martin et al., 1988; Pierotti et al., 1991). In our model, we did not find any correlations between the degree of functional recovery and numbers of motoneurons in the lumbar spinal cord (data not shown). The question of motoneuronal numbers and their functional significance is very important in the light of recent studies in which motoneuron replacement therapy was suggested as a potential treatment after SCI (for review see Silani et al., 2004).

5.1.2 Interneurons

Similar to ChAT$^+$ motoneurons, we detected a large loss of PV$^+$ interneurons in both the ventral (-40%) and the dorsal (-50%) horn of injured spinal cords. At the same time, as compared with intact mice, the overall number on NeuN$^+$ neurons was reduced by 23% in the ventral horn, while the difference of -10% in the dorsal horn was not statistically significant. Since loss of PV$^+$ interneuron after SCI was more pronounced that the changes in the entire neuronal population in both the ventral and dorsal horn, our data are consistent with the idea of a specific vulnerability of the PV$^+$ interneurons, similar to motoneurons after SCI. As for motoneurons, our data does not allow to

identify the reason for PV$^+$ cell loss, cell death or downregulation of PV expression. PV levels vary greatly between interneuronal subpopulations in the intact spinal cord (Fig. 1C,D; also Alvarez et al., 2005). It is possible that cells expressing low levels of PV would turn into PV negative cells after injury. However, such large decreases in cell numbers (>40%) observed here are not easily attributable to marker expression downregulation alone, so it is possible that PV$^+$ interneurons are also affected by cell death. It would be very difficult to design an experiment that would give a straightforward answer to the question why less PV$^+$ cells are present in the injured spinal cord, since no other cell marker can be used to visualize the entire PV$^+$ cell population. Nevertheless, it can be proposed that downregulation of PV may by itself is a sign of degeneration of these neurons. Evidence exists that PV may protect neurons from cell death induced by glutamate excitotoxicity. Transgenic mice overexpressing PV have decreased injury-induced motoneuronal cell death (Dekkers et al., 2004). Similar to motoneurons, PV plays a very important role in interneuron homeostasis and the levels of its expression dynamically change upon ischaemic injury (Tortosa and Ferrer, 1993). PV-containing interneurons of striatum are more susceptible to degeneration in the ischaemic stroke injury model, compared with other interneuronal populations (Chesselet et al., 1990). In the hippocampus, interneurons are not susceptible to cell death after transient brain ischemia, but display various ultrastructural degenerative changes (Fukuda et al., 1993). Overall, our finding of reduced numbers of PV$^+$ interneurons in the mouse lumbar spinal cord after thoracic compression is novel in this injury paradigm, and may have potentially important pathophysiological implications.

5.1.3 Sensory neurons in the dorsal horn

Stereological counting of dorsal horn neurons in lumbar spinal cords did not reveal statistically significant differences before and after injury. Since the number of PV$^+$ interneurons in the dorsal horns was reduced by half, we conclude that the number of dorsal horn projection neurons which conduct sensory information from dorsal root ganglia to higher brain centers was not reduced after injury. This finding is puzzling, considering that axons of these neurons are directly affected at the lesion site. Afferent input to these neurons is unaffected by SCI. It is well documented across species and injury models that, upon peripheral nerve lesion, dorsal horn neurons undergo transsynaptic degeneration and death (Knyhar Csillik et al., 1989; Marsala et al., 1995;

Hama et al., 1996). Our results suggest that although dorsal horn neurons are very sensitive to deafferentiation after peripheral nerve lesion, they are quite robust in response to injury of their own axons. Another explanation could be that our observation period (6 weeks after injury) was not long enough to detect late-occurring cell death. Even if the number of sensory spinal cord neurons is not affected, their function is definitely altered, since chronic pain after injury is one of its most prominent symptoms after SCI (for review see Deumens et al., 2008).

5.2 Glial reaction to spinal cord injury

5.2.1 Astrocytes

The most extensively explored topic in the field of CNS regeneration is the "glial scar". Unlike for microglia, however, there is no consensus about how generalized the astrogliosis is after injury. Upon injury astrocytes at the lesion site undergo hypertrophy and proliferation, characterized by upregulation of GFAP and many other molecules (see, for example, Landis, 1994). Interestingly, the astrocyte response to injury is much milder in neonatal rats than in adults (Barrett et al., 1984). Reactive astrocytes appear larger and have more processes than those in the uninjured CNS (Schwab and Bartholdi, 1994). Several studies report astrocyte proliferation in the rat lumbar spinal cord up to 4 weeks after lower thoracic transection (Barrett et al., 1981, 1984). These studies have, however, estimated only density of GFAP immunostaining and not cell numbers using stereological methods for quantification. Using stereology, we found that the S-100$^+$ cell density in the mouse lumbar spinal cord grey matter is reduced after injury (data not shown). However, since the volume of the grey matter is reduced, over the total number of astrocytes in the lumbar spinal cord is not changed after SCI. This does not suggest that astrocytes distal to lesion site are unaffected by injury, but is a strong indication that there is not much astrocyte proliferation away from the site of injury. There is, however, evidence that some features of astrocytes in the lumbar spinal cord are affected by injury, for example Jakovcevski et al. (2007) found elevated GFAP levels as measured by Western blots in the lumbar spinal cords of injured CHL1+/+ and CHL1-/- mice compared to uninjured mice.

5.2.2 Oligodendrocytes

Early studies from the beginning of the 20th century suggested that demyelination plays an important role in the pathology of compressive SCI (Holmes, 1906). It was in

this seminal publication that Holmes suggested that loss of myelin interfered with conduction in ascending and descending axons in the white matter (Holmes, 1906). Recent studies confirmed that demyelination constitutes a very important part of the pathology of experimental SCI (Gledhill et al., 1973; Totoiu and Keirstead, 2005). Detailed electron microscopy studies have shown that the predominant pathology following mild compressive and contusive injury is demyelination of intact axons (Gledhill et al., 1973; Bresnahan, 1978; Blight, 1983). Demyelination starts within the first 24 hours after injury and increases during the first two weeks. Evidence of remyelination is seen at 3 weeks (Gledhill and McDonald, 1977; Harrison and McDonald, 1977). More extensive remyelination is observed around smaller lesions (Harrison and McDonald, 1977). At least in part the remyelination is carried out by oligodendrocytes, although Schwann cell remyelination also plays a role after SCI, specifically around dorsal root entry zones, where Schwann cells invade the spinal cord (Gledhill and McDonald, 1977; Bartlett Bunge., 1994). In the light of the demyelination/remyelination dynamics after SCI, the time-point of analysis in our study was late in the sense that the proliferation of oligodendrocytes is completed by that time-point, while both demyelination and remyelination proceed. Thus, an almost 50% decrease in the density of the CNP$^+$ oligodendrocytes in the white matter would indicate that, due to the severity of lesion in our paradigm, there is a significant deficit in myelination 6 weeks after injury. At the same time, we found no changes, as compared to intact mice, in the number of gray matter oligodendrocytes. The differential response of the oligodendrocytes in the white and the gray matter may be explained by the assumption that oligodendrocytes in the gray matter are less susceptible to damage or proliferate more extensively in the early phase of SCI compared to white matter oligodendrocytes. Considering that CNP antibodies label some oligodendrocyte precursors cells (O4+CNP+), as well as all mature oligodendrocytes in mice (Godfraind et al., 1989), it is also possible that a more vigorous proliferation of oligodendrocyte progenitors in the gray matter masks a relatively small loss in oligodendrocytes. Since most of the literature published on oligodendrocytes after SCI deals only with the white matter, this is to our knowledge the first report about numbers of grey matter oligodendrocytes in the chronic phase of SCI. The loss oligodendrocytes in the white matter is apparently of functional importance since transplantation of myelination-competent cells after SCI is beneficial (Blackmore, 1977; Faulkner and Keirstead, 2005; Keirstead et al., 2005).

5.2.3 Microglia

It is a well-documented fact that after CNS injury the microglial cell proliferation is not restricted to the site of injury (Streit et al., 1999; Ladeby et al., 2005). Our finding of dramatically increased numbers of microglial cells in lumbar spinal cords upon lower thoracic injury is, thus, not surprising. Furthermore, our observation of microglial "clusters", evident only in the white matter, indicates that a substantial amount of debris is present in the white matter 6 weeks after injury, most likely due to ongoing axonal and myelin degeneration.

In the normal adult CNS, microglial cell numbers are kept constant by a balance between natural cell loss and resident microglia proliferation or recruitment of bone marrow cells through the intact blood-brain barrier (Lawson et al., 1992). It has been estimated that in the intact brain microglia comprise 5-12% of non-neuronal cells, depending on the brain region (Lawson et al., 1990). Previous data about the spinal cord suggest that glia, essentially astrocytes and microglia, outnumber neurons (Kuffler et al., 1984). Our data show that astrocytes, oligodendrocytes and microglia comprise each about 1/3 of the entire glia population within the intact spinal cord. The total number of glial cells is approximately equal to the total number of NeuN$^+$ neurons. Although understanding of the function of the resting microglia is still limited, there is a large body of research on activated microglia. Microglial activation is characterized by morphological transformation, induction of the expression of a wide range of myeloid markers and the acquisition of a phagocytic phenotype (Streit et al., 1999). Since we found that numbers of microglia were increased after injury, the implication is that a considerable microglial proliferation occurrs in response to injury. It is unclear whether the proliferation and activation of microglia in the lumbar spinal cord have beneficial or adverse effects on the functional recovery and regeneration processes. For example, in two different injury paradigms, irreversible and reversible facial nerve injury, Streit and Kreutzberg (1988) have found that microglia proliferate and surround injured motoneurons. In the case of irreversible injury, the microglial cells become rounded brain macrophages and digest the dying neurons (Streit and Kreutzberg, 1988). After reversible injury, however, activated microglia is involved in displacement of afferent nerve endings around motoneuron cell bodies ("synaptic stripping", Kreutzberg, 1966). Synaptic elimination by microglia may be important for the recovery after compressive SCI, since it has been shown that excitability of motoneurons in the lumbar spinal cord correlates with the degree of functional recovery (Lee et al., 2009). It would be

interesting to investigate in our severe compression injury model whether activated microglia in the lumbar spinal cord is mainly clearing cell debris or, in addition or predominantly, is involved in synaptic plasticity and thus beneficial for regenerative processes. One way to address this question would be to study injured spinal cords at the ultrastructural level, looking specifically into the amount of cell death and positioning of microglial cells and their processes with regard to neurons and synapses. Another way to address the question whether the microglial response after SCI is beneficial or adverse would be to compare functional recovery in microglial cell-deficient transgenic mice and wild-type mice (Heppner et al., 2005).

5.3 The effect of CHL1 ablation on cell populations in the spinal cord

5.3.1 The effect of CHL1 ablation on the formation of spinal cord cell populations

Although CHL1-/- mice have apparently normal brains and spinal cords, numerous abnormalities have been reported in their behavior, as well as subtle structural abnormalities of their brains (Irintchev et al., 2004; Nikonenko et al., 2006; Morellini et al., 2007; Jakovcevski et al., 2009). Most prominently, these mice have increased numbers of PV^+ interneurons in the hippocampus and the cerebral cortex at young age (1 months) compared with CHL1+/+ littermates, and these numbers decrease during aging, to become abnormally low in the hippocampus later in adulthood (6-12 months) (Nikonenko et al., 2006; Thilo, 2006). Another prominent finding in CHL1-/- mice is the age- and region-specific increase in microglial cell densities, in 1-2-month-old hippocampi compared with wild-types (Thilo, 2006). These findings are not present in 3-month-old spinal cords of CHL1-/- mice, and their cell composition is very similar to CHL1+/+ mice. Thus, we conclude that CHL1 is not essential for the formation of spinal cord cell populations, or that other molecules in CHL1-/- mice compensate its function. This is corroborated by the observations that CHL1 mice walk normally and show no apparent sensory abnormalities (Jakovcevski et al., 2007; Morellini et al., 2007).

5.3.2 The effect of CHL1 ablation on cell population in injured spinal cords

The most important finding of a previous study on the role of CHL1 in SCI was the up-regulation of CHL1 by astrocytes at the lesion site, leading to increased astrocyte activation and adverse effect on regeneration (Jakovcevski et al., 2007). The number of astrocytes in the lumbar spinal cord after injury is unchanged compared with intact mice

of both genotypes (CHL1-/- and CHL1+/+). This finding is in agreement with a previous study, in which we observed no difference in the amount of GFAP, assessed by Western blots, in the lumbar spinal cords between CHL1+/+ and CHL1-/- mice 7 days after thoracic injury (Jakovcevski et al., 2007). Also in agreement with the previous study was the finding that numbers of Iba1^{+} microglia, oligodendrocytes and neurons were very similar between the genotypes. There was, however, one notable exception. Number of PV[+] interneurons was decreased upon injury in both CHL1+/+ and CHL1-/-, but in CHL1-/- mice it decreased to a larger degree. The difference in numbers of PV^{+} cells between the genotypes after injury was by 30% in both dorsal and ventral horns, but it was statistically significant only in ventral horns. This speaks for higher vulnerability of PV[+] interneurons in CHL1-/- mice than in their wild-type littermates, which is in congruence with our previous observations in the hippocampus (Thilo, 2006). The recovery of motor function is surprisingly better in CHL1-/- mice than in their wild-type littermates (Jakovcevski et al., 2007). The underlying mechanisms probably involve better axonal regeneration and sprouting in the lumbar spinal cord after injury, due to the absence of detrimental CHL1-CHL1 homophilic interactions in the mutants. In addition, motoneuronal excitability after injury, as estimated by H-reflex analysis, is higher in CHL1-/- than in CHL1+/+ mice (Lee et al., 2009). Alterations in the cellular composition of the lumbar spinal cord after injury, however, are not among the factors that can explain the difference in the degree of recovery in CHL1-/- and CHL1+/+ mice.

5.4 Conclusion

This work adds to the knowledge about morphological consequences of SCI. Changes in the cellular composition of the lumbar spinal cord after compression of the thoracic spinal cord in mice are described for the first time in a comprehensive manner. The results show that, irrespective of genotype, both neuronal and glial cell populations in the lumbar spinal cord, as well as the spinal cord volume, are significantly affected 6 weeks after injury

Unlike in the hippocampus or cerebellum, the CHL1 deficiency has little effect on the size of neuronal and glial cell populations in the intact spinal cord (Nikonenko et al., 2006; Jakovcevski et al., 2009). After injury, changes observed in the lumbar spinal cord volume and the neuronal and glial populations in the wild-type mice were very similar to those in CHL1-/- mice. Therefore, the previously reported enhanced

recovery of motor function after SCI in CHL1-/- mice as compared with CHL1+/+ mice cannot be explained by genotype-specific changes in cell population numbers.

Some of the important future directions prompted by our study would include examining cell death and proliferation in the lumbar spinal cord after injury. This could be helpful for designing future therapeutic strategies such as utilization of neuroprotective agents and cell-replacement therapies.

6 SUMMARY

Poor recovery from severe injuries of the spinal cord in adult mammals including humans is primarily attributed to the low intrinsic potential of CNS neurons to regenerate their severed axons and to regeneration-inhibiting factors in and around the site of injury. To what degree changes in the spinal cord distal to the site of injury, such as, for example, neuronal death and glial cell loss or proliferation, contribute to the pathology after SCI is poorly understood. Here we addressed this question utilising a well-established injury paradigm, severe low-thoracic compression injury in adult mice. Using immunohistochemical cell markers and stereology, we estimated total numbers of different neuronal and glial cell types in the lumbar spinal cord 6 weeks after SCI, a time-point at which the very limited spontaneous functional recovery in this model has almost reached a maximum. Analysis of uninjured and injured C57BL/6J mice revealed dramatic injury-related structural alterations in the lumbar spinal cord. Gray and white matter volumes were reduced by one-third compared with normal. The number of all neurons (NeuN$^+$) and that of ChAT$^+$ motoneurons in the ventral horn were reduced, compared with uninjured mice (by 24% and 35%, respectively) and fewer PV$^+$ interneurons were detectable in both the ventral (-40%) and dorsal horn (-50%). While SCI did not affect the S-100$^+$ astrocytes, the CNPase$^+$ oligodendrocytes in the white matter were reduced in number by 32%. And finally, a remarkable degree of microgliosis was found in the ventral horn (90% more Iba1$^+$ microglial cells compared with uninjured mice). Similar injury-related alterations were found in mice deficient in the expression of the cell adhesion molecule CHL1 (close homologue of L1), mice previously shown to recover some functional abilities better than wild-type mice after compression SCI. While these results cannot explain the different outcomes in wild-type and CHL1-deficient mice, they suggest that neuronal and glial changes in the distal spinal cord are factors limiting, irrespective of genotype, recovery of function after SCI. In particular, reduction in the numbers of ChAT$^+$ motoneurons and PV$^+$ interneurons, whether due to reduced expression of ChAT and PV, molecules crucial for normal cell functions, and/or to cell death, must have consequences. Also the finding of a reduced number of CNPase$^+$ oligodendrocytes in the white matter is in line with the notion that oligodendrocyte death and axonal de-/hypomyelination play a central role in SCI pathology. The results of this study warrant further investigations on the contribution of specific cell alterations in the distal spinal cord to disabilities after SCI.

7 REFERENCES

Ackery A, Tator C, Krassioukov A (2004) A global perspective on spinal cord injury epidemiology. J Neurotrauma 21:1355-70.

Alvarez FJ, Jonas PC, Sapir T, Hartley R, Berrocal MC, Geiman EJ, Todd AJ, Goulding M (2005) Postnatal phenotype and localization of spinal cord V1 derived interneurons. J Comp Neurol 493:177-192.

Apostolova I, Irintchev A, Schachner M (2006) Tenascin-R restricts posttraumatic remodeling of motoneuron innervation and functional recovery after spinal cord injury in adult mice. J Neurosci 26:7849-7859.

Azari MF, Profyris C, Zang DW, Petratos S, Cheema SS (2005) Induction of endogenous neural precursors in mouse models of spinal cord injury and disease. Eur J Neurol 12:638-48.

Bareyre FM, Kerschensteiner M, Raineteau O, Mettenleiter TC, Weinmann O, Schwab ME (2004) The injured spinal cord spontaneously forms a new intraspinal circuit in adult rats. Nat Neurosci 7:269-77.

Barrett CP, Donati EJ, Guth L (1984) Differences between adult and neonatal rats in their astroglial response to spinal injury. Exp Neurol 84:374-385.

Barrett CP, Guth L, Donati EJ, Krikorian JG (1981) Astroglial reaction in the gray matter lumbar segments after midthoracic transection of the adult rat spinal cord. Exp. Neurol 73:365-377.

Bartlett Bunge M, Holets VR, Bates ML, Clarke TS, Watson BD (1994) Characterization of pathochemically induced spinal cord injury in the rat by light and electron microscopy. Exp Neurol 127:76-93.

Beattie MS, Bresnahan JC, Komon J, Tovar CA, Van Meter M, Anderson DK, Faden AI, Hsu CY, Noble LJ, Salzman S, Young W (1997) Endogenous repair after spinal cord contusion injuries in the rat. Exp Neurol 148:453-63.

Bjugn R, Nyengaard JR, Rosland JH (1997) Spinal cord transection – no loss of distal ventral horn neurons. Exp Neurol 148: 179-186.

Blakemore WF (1977) Remyelination of CNS axons by Schwann cells transplanted from the sciatic nerve. Nature 266:68–69.

Blight, AR (1983) Cellular morphology of chronic spinal cord injury in the cat: analysis of myelinated axonas by line-sampling. J Neurosci 10:521-543.

Bracken MB, Freeman DH Jr, Hellenbrand K (1981) Incidence of acute traumatic hospitalized spinal cord injury in the United States, 1970-1977. Am J Epidemiol 113:615-22.

Bresnahan JC (1978) An electron-microscopic analysis of axonal alterations following blunt contusion of the spinal cord of the rhesus monkey (Macaca mulatta). J Neurol Sci 37:59-82.

Bunge RP, Puckett WR, Becerra JL, Marcillo A, Quencer RM (1993) Observations on the pathology of human spinal cord injury. A review and classification of 22 new cases with details from a case of chronic cord compression with extensive focal demyelination. Adv Neurol 59:75-89.

Bunge RP (1994) The role of the Schwann cell in trophic support and regeneration. J Neurol 242:S19-21.

Bush TG, Puvanachandra N, Horner CH, Polito A, Ostenfeld T, Svendsen CN, Mucke L, Johnson MH, Sofroniew MV (1999) Leukocyte infiltration, neuronal degeneration, and neurite outgrowth after ablation of scar-forming, reactive astrocytes in adult transgenic mice. Neuron 23:297-308.

Celio MR (1986) Parvalbumin in most gamma-aminobutyric acid-containing neurons of the rat cerebral cortex. Sience 231:995-7.

Chaisuksunt V, Campbell G, Zhang Y, Schachner M, Lieberman AR, Anderson PN (2000a) The cell recognition molecule CHL1 is strongly upregulated by injured and regenerating thalamic neurons. J Comp. Neurol 425:382-392.

Chaisuksunt V, Zhang Y, Anderson PN, Campbell G, Vaudano E, Schachner M, Lieberman AR (2000b) Axonal regeneration from CNS neurons in the cerebellum and brainstem of adult rats: Correlation with the patterns of expression and distribution of messenger RNAs for L1, CHL1, c- jun and growth associated protein 43. J Neurosci 100:87-108.

Chen S, Mantei L, Dong L, Schachner M (1999) Prevention of neuronal cell death by neural adhesion molecules L1 and CHL1. J Neurobiol 38:428-439.

Chen QY, Chen Q, Feng GY, Lindpaintner K, Chen Y, Sun X, Chen Z, Gao Z, Tang J, He L (2005) Case-control association study of the close homologue of L1 (CHL1) gene and schizophrenia in the Chinese population. Schizophr Res 73:269-74.

Chesselet MF, Gonzales C, Lin CS, Polsky K, Jin BK (1990) Ischemic damage in the striatum of adult gerbils: relative sparing of somatostatinergic and cholinergic interneurons contrasts with loss of efferent neurons. Exp Neurol 110:209–218.

Cowan RJ, Maynard CD, Lassiter KR (1970) Technetium-99m pertechnetate brain scans in the detection of subdural hematomas: a study of the age of the lesion as related to the development of a positive scan. J Neurosurg 32:30-34.

Crowe MJ, Bresnahan JC, Shuman SL, Masters JN, Beattie MS (1997) Apoptosis and delayed degeneration after spinal cord injury in rats and monkeys. Nat Med 3:73-6.

Cunningham BA (1995) Cell adhesion molecules as morphoregulators. Curr Opin Cell Biol 7:628-633.

Curtis R, Green D, Lindsay RM, Wilkin GP (1993) Up-regulation of GAP-43 and growth of axons in rat spinal cord after compression injury. J Neurocytol 22:51-64.

da Paz AC, Beraldo PS, Almeida MC, Neves EG, Alves CM, Khan P (1992) Traumatic injury to the spinal cord. Prevalence in Brazilian hospitals. Paraplegia 30:636-40.

Dekkers J, Bayley P, Dick JRT, Schwaller B, Berchtold MW, Greensmith L (2004) Over-expression of parvalbumin in transgenic mice rescues motoneurons from injury-induced cell death. J Neurosci 123:459-466.

Demyanenko GP, Anton E, Schachner M, Feng G, Sanes J, Maness PF (2004) Close homolog of L1 modulates area-specific neuronal positioning and dendrite orientation in the cerebral cortex. Neuron 44: 423-437.

Deumens R, Joosten EA, Waxman SG, Hains BC (2008) Locomotor dysfunction and pain: the scylla and charybdis of fiber sprouting after spinal cord injury. Mol Neurobiol 37:52-63.

Dincer F, Oflazer A, Beyazova M, Celiker R, Basgöze O, Altioklar K (1992) Traumatic spinal cord injuries in Turkey. Paraplegia 30:641-6.

Dong Teng Y, Mocchetti I, Taveira-DaSilva A, Gillis R, Wrathall J (1999) Basic fibroblast growth factor increases long-term survival of spinal motor neurons and improves respiratory function after spinal cord injury. J Neurosci 19:7037-7047.

Eidelberg E, Nguyen LH, Polich R, Walden JG (1989) Transsynaptic degeneration of motoneurones caudal to spinal cord lesions. Brain Res Bull 22:39-45.

Engesser-Cesar C, Ichiyama RM, Nefas AL, Hill MA, Edgerton VR, Cotman CW, Anderson AJ (2007) Wheel running following spinal cord injury improves locomotor recovery and stimulates serotonergic fiber growth. Eur J Neurosci 25 :1931-9.

Faulkner JR, Herrmann JE, Woo MJ, Tansey KE, Doan NB, Sofroniew MV (2004) Reactive astrocytes protect tissue and preserve function after spinal cord injury. J Neurosci 24:2143-55.

Faulkner J, Keirstead HS (2005) Human embryonic stem cell-derived oligodendrocyte progenitors for the treatment of spinal cord injury. Transplant. Immunol 15:131-142.

Frints SG, Marynen P, Hartmann D, Fryns JP, Steyaert J, Schachner M, Rolf B, Craessaerts K, Snellinx A, Hollanders K, D'Hooge R, De Deyn PP, Froyen G (2003) CALL interrupted in a patient with non-specific mental retardation: gene dosage-dependent alteration of murine brain development and behavior. Hum Mol Genet 12: 1463-1474.

Fukuda T, Nakano S, Yoshiya I, Hashimoto PH (1993) Persistent degenerative state of non-pyramidal neurons in the CA1 region of the gerbil hippocampus following transient forebrain ischemia. J Neurosci 53:23-38.

Gledhill RF, Harrison BM, McDonald WI (1973) Demyelination and remyelination after acute spinal cord compression. Exp Neurol 38:472-487.

Gledhill RF, McDonald WI (1977) Morphological characteristics of central demyelination and remyelination: a single-fiber study. Ann Neurol 1:522-560.

Godfraind C, Friedrich VL, Holmes KV, Dubois-Dalcq M (1989) In vivo analysis of glial cell phenotypes during viral demyelinating disease in mice. J Cell Biol 109:2405-2416.

Hama A, Pappas TGD, Sagen J (1996) Adrenal medullary implants reduce transsynaptic degeneration in the spinal cord of rats following chronic constriction nerve injury. Exp Neurol 137:81-93.

Harrison BM, McDonald WI (1977) Remyelination after transient experimental compression of the spinal cord. Ann Neurol 1:542-551.

Hart C, Williams E (1994) Epidemiology of spinal cord injuries: a reflection of changes in South African society. Paraplegia 32:709-14.

Heppner FL, Greter M, Marino D, Falsig J, Raivich G, Hövelmeyer N, Waisman A, Rülicke T, Prinz M, Priller J, Becher B, Aguzzi A (2005) Experimental autoimmune encephalomyelitis repressed by microglial paralysis. Nat Med 11:146-152.

Hill CE, Beattie MS, Bresnahan JC (2001) Degeneration and sprouting of identified descending supraspinal axons after contusive spinal cord injury in the rat. Exp Neurol 171:153-69.

Hillenbrand R, Molthagen M, Montag D, Schachner M (1999) The close homologue of neural adhesion molecule L1 (CHL1): Patterns of expression and promotion of neurite outgrowth by heterophilic interactions. Eur J Neurosci 11: 813-826.

Holm J, Hillenbrand R, Steuber V, Bartsch U, Moos M, Lübbert H, Montag D, Schachner M (1996) Structural features of a close homologue of L1 (CHL1) in the mouse: a new member of the L1 family of neural recognition molecules. Eur J Neurosci 8: 1613-1629.

Holmes G (1906) On the relation between loss of function and structural change in focal lesions of the central nervous system, with special reference to secondary degeneration. J Brain 29:514-523.

Hoque MF, Grangeon C, Reed K (1999) Spinal cord lesions in Bangladesh: an epidemiological study 1994 - 1995. Spinal Cord 37:858-61.

Howard CV, Reed MG (1998) Surface-weighted star volume: concept and estimation. J Microsc 190:350-6.

Imai Y, Kohsaka S (2002) Intracellular signaling in M-CSF-induced microglia activation: role of Iba1. Glia 40:164-74.

Irintchev A, Koch M, Needham LK, Maness P, Schachner M (2004) Impairment of sensorimotor gating in mice deficient in the cell adhesion molecule L1 or its close homologue, CHL1. Brain Res 1029:131-4.

Irintchev A, Rollenhagen A, Tronscoso E, Kiss JZ, Schachner M (2004a) Structural and functional aberrations in the cerebral cortex of tenascin-C deficient mice. Cereb Cortex 15:950-62.

Irintchev A, Rollenhagen A, Troncoso E, Kiss JZ, Schachner M (2005) Structural and functional aberrations in the cerebral cortex of tenascin-C deficient mice. Cereb Cortex 15:950-62.

Jakovcevski I, Wu J, Karl N, Leshchyns'ka I, Sytnyk V, Chen J, Irintchev A, Schachner M (2007) Glial scar expression of CHL1, the close homolog of the adhesion molecule L1, limits recovery after spinal cord injury. J Neurosci 27: 7222-7233.

Jakovcevski I, Siering J, Hargus G, Karl N, Hoelters L, Djogo N, Yin S, Zecevic N, Schachner M, Irintchev A (2009) Close homologue of adhesion molecule L1 promotes survival of Purkinje and granule cells and granule cell migration during murine cerebellar development. J Comp Neurol 513:496-510.

Jones TB, McDaniel EE, Popovich PG (2005) Inflammatory-mediated injury and repair in the traumatically injured spinal cord. Curr Pharm Des 11:1223-36.

Kakulas BA (1999) The applied neuropathology of human spinal cord injury. Spinal Cord 37:79-88.

Keirstead HS, Nistor G, Bernal G, Totoiu M, Cloutier F, Sharp K, Steward O (2005) Human embryonic stem cell-derivied oligodendrocyte progenitor cell transplants remyelinate and restore locomotion after spinal cord injury. J Neurosci 25:4694-4705.

Knyihar Csillik E, Rakic P, Csillik B (1989) Transneuronal degeneration in the Rolando substance of the primate spinal cord evoked by axotomy-induced transganglionic degenerative atrophy of central primary sensory terminals. Cell Tissue Res 258:515-525.

Krassioukov AV, Furlan JC, Fehlings MG (2003) Medical co-morbidities, secondary complications, and mortality in elderly with acute spinal cord injury. J Neurotrauma 20:391-9.

Kreutzberg GW (1966) Autoradiographische Untersuchung über die Beteiligung von Gliazellen an der axonalen Reaktion im Facialiskern der Ratte. Acta Neuropathol 7:149-161.

Kuffler SW, Nicholls JG, Martin AR (1984) Physiology of neuroglial cells. In: From neuron to brain, pp 323-360. Sunderland, MA: Sinauer Associates Inc.

Ladeby R, Wirenfeldt M, Garcia-Ovejero D, Fenger C, Dissing-Olesen L, Dalmau I, Finsen B (2005) Microglial cell population dynamics in the injured adult central nervous system. J Brain Res Brain Res Rev. 48:196-206.

Landis DM (1994) The early reactions of non-neuronal cells to brain injury. Annu Rev Neurosci 17:133-151.

Lawson LJ, Perry VH, Gordon S (1992) Turnover of resident microglia in the normal adult mouse brain. J Neurosci 48:405-415.

Lawson LJ, Perry VH, Dri P, Gordon S (1990) Heterogeneity in the distribution and morphology of microglia in the normal adult mouse brain. J Neurosci 39:151-170.

Lee HJ, Jakovcevski I, Radonjic N, Hoelters L, Schachner M, Irintchev A (2009) Better functional outcome of compression spinal cord injury in mice is associated with enhanced H-reflex responses. J Exp Neurol 216:365-374.

Levy LF, Makarawo S, Madzivire D, Bhebhe E, Verbeek N, Parry O (1998) Problems, struggles and some success with spinal cord injury in Zimbabwe. Spinal cord 36:213-8.

Lieberoth A, Splittstoesser F, Katagihallimath N, Jakovcevski I, Loers G, Ranscht B, Karagogeos D, Schachner M, Kleene R (2009) Lewis(x) and alpha2,3-sialyl glycans and their receptors TAG-1, Contactin, and L1 mediate CD24-dependent neurite outgrowth. J Neurosci 29:6677-90.

Marsala J, Sulla, I, Jalc P, Orendacova J (1995) Multiple protracted cauda equina constrictions cause deep derangement in the lumbosacral spinal cord circuitry in the dog. Neurosci Lett 193:97-100.

Martin TP, Bondine Fowler S, Edgerton VR (1988) Coordination of electromechanical and metabolic properties of cat soleus motor units. Am J Physiol 255:C684-693.

Martins F, Freitas F, Martins L, Dartigues JF, Barat M (1998) Spinal cord injuries-epidemiology in Portugal's central region. Spinal cord 36:574-8.

McBride RL, Feringa ER (1992) Ventral horn motoneurons 10, 20 and 52 weeks after T-9 spinal cord transection. Brain Res Bull 28: 57-60.

McKinley WO, Kolakowsky SA, Kreutzer JS (1999) Substance abuse, violence, and outcome after traumatic spinal cord injury. Am J Phys Med Rehabil 78:306-12.

Montag-Sallaz M, Schachner M, Montag D (2002) Misguided axonal projections, neural cell adhesion molecule 180 mRNA upregulation and altered behavior in mice deficient for the close homolog of L1. Mol Cell Biol: 7967-7981.

Morellini F, Lepsveridze E, Kähler B, Dityatev A, Schachner M (2006) Reduced reactivity to novelty, impaired social behavior, and enhanced basal synaptic excitatory activity in perforant path projections to the dentate gyrus in young adult mice deficient in the neural cell adhesion molecule CHL1. Mol Cell Neurosci 34:121-36.

Nakamura M, Okada S, Toyama Y, Okano H (2005) Role of IL-6 in spinal cord injury in a mouse model. Clin Rev Allergy Immunol 28:197-204.

Nikonenko AG, Sun M, Lepsveridze E, Apostolova I, Petrova I, Irintchev A, Dityatev A, Schachner M (2006) Enhanced perisomatic inhibition and impaired long-term potentiation in the CA1 region of juvenile CHL1-deficient mice. Eur J Neurosci 23:1839-52.

O'Connor P (2002) Injury to the spinal cord in motor vehicle traffic crashes. Accid Anal Prev 34:477-85.

Okado N, Oppenheim RW (1984) Cell death of motoneurons in the chick embryo spinal cord. The loss of motoneurons following removal of afferent inputs. J Neurosci 4:1639-1652.

Pierotti DJ, Roy RR, Bodine Fowler SC, Hodgson JA, Edgerton VR (1991) Mechanical and morphological properties of clinically inactive cat tibialis anterior motor units. J Physiol 444:175-192.

Raineteau O, Schwab ME (2001) Plasticity of motor systems after incomplete spinal cord injury. Nat Rev Neurosci 2:263-73.

Raineteau O, Fouad K, Bareyre FM, Schwab ME (2002) Reorganization of descending motor tracts in the rat spinal cord. Eur J Neurosci 16:1761-71.

Rathjen FG (1991) Neural cell contact and axonal growth. Curr Opin Cell Biol 3:992-1000.

Rutishauser U (1993) Adhesion molecules of the nervous system. Cell Opin Neurobiol 3:709-15.

Sakurai K, Migita O, Toru M, Arinami T (2002) An association between a missense polymorphism in the close homologue of L1 (CHL1, CALL) gene and schizophrenia. Mol Psych 7:412-415.

Schachner M (1991) Cell surface recognition and neuron-glia interactions. Ann N Y Acad Sci 633:105-12.

Schachner M (1994) Neural recognition molecules in disease and regeneration. Curr Opin Neurobiol 4:726-34.

Schwab ME, Bartholdi D (1994) Degeneration and regeneration of axons in the lesioned spinal cord. Physiol Rev 76:310-370.

Sekhon LH, Fehlings MG (2001) Epidemiology, demographics, and pathophysiology of acute spinal cord injury. Spine 26:S2-12.

Silani V, Cova L, Corbo M, Ciammola A, Polli E (2004) Stem-cell therapy for amyotrophic lateral sclerosis. Lancet 364:200-202.

Silver J, Miller JH (2004) Regeneration beyond the glial scar. Nat Rev Neurosci 5:146-56.

Simova O, Irintchev A, Mehanna A, Liu J, Dihné M, Bächle D, Sewald N, Loers G, Schachner M (2006) Carbohydrate mimics promote functional recovery after peripheral nerve repair. Ann Neurol 60:430-7.

Sofroniew MV and Schrell U (1982) Long-term storage and regular repeated use of diluted antisera in glass staining jars for increased sensitivity, reproducibility, and convenience of single- and two-color light microscopic immunocytochemistry. J Histochem Cytochem 30:504-511.

Streit WJ, Walter SA, Pennell NA (1999) Reactive microgliosis. Prog. Neurobiol 57:563-581.

Streit WJ, Kreutzberg GW (1988) The response of endogenous glial cells to motor neuron degeneration induced by toxin ricin. J Comp Neurol 268:248-263.

Tacke R, Moos M, Teplow DB, Früh K, Scherer H, Bach A, Schachner M (1987) Identification of cDNA clones of the mouse neural cell adhesion molecule L1. Neurosci Lett 82:89-94.

Tator CH, Duncan EG, Edmonds VE, Lapczak LI, Andrews DF (1993) Complications and costs of management of acute spinal cord injury. Paraplegia 31:700-14.

Tator CH (1995) Update on the pathophysiology and pathology of acute spinal cord injury. Brain Pathol 5:407-13.

Tator CH, Carson JD, Cushman R (2000) Hockey injuries of the spine in Canada, 1966-1996. CMAJ 162:787-8.

Thilo BE (2006) Age dependent and region-specific alterations in the brain of CHL1 deficient mice: an emerging animal-based model of schizophrenia. Inaugural Dissertation, University of Hamburg.

Thuret S, Moon LD, Gage FH (2006) Therapeutic interventions after spinal cord injury. Nat Rev Neurosci 7:628-43.

Totoiu MO, Keirstead HS (2005) Spinal cord injury is accompanied by chronic progressive demyelination. J Comp Neurol 486:373-83.

Tortosa A, Ferrer I (1993) Parvalbumin immunoreactivity in the hippocampus of the gerbil after transient forebrain ischaemia: a qualitative and quantitative sequential study. J Neurosci 55:33-43.

Velardo MJ, Burger C, Williams PR, Baker HV, López MC, Mareci TH, White TE, Muzyczka N, Reier PJ (2004) Patterns of gene expression reveal a temporally orchestrated wound healing response in the injured spinal cord. J Neurosci 24:8562-76.

Wolf HK, Buslei R, Schmidt-Kastner R, Schmidt-Kastner PK, Pietsch T, Wiestler OD, Blümcke I (1996) NeuN: a useful neuronal marker for diagnostic histopathology. J Histochem Cytochem. 44:1167-71.

Yamamoto S, Yamamoto N, Kitamura T, Nakamura K, Nakafuku M (2001) Proliferation of parenchymal neural progenitors in response to injury in the adult rat spinal cord. Exp Neurolog 172:115-27.

Yang H, Lu P, McKay HM, Bernot T, Keirstead H, Steward O, Gage FH, Edgerton VR, Tuszynski MH (2006) Endogenous neurogenesis replaces oligodendrocytes and astrocytes after primate spinal cord injury. J Neurosci 26:2157-66.

Young IJ (1966) Morphological and histochemical studies of partially and totally deafferented spinal cord segments. Exp Neurol 14:238-248.

Zhang Y, Roslan R, Lang D, Schachner M, Lieberman AR, Anderson PN (2000) Expression of CHL1 and L1 by neurons and glia following sciatic nerve and dorsal root injury. Mol Cell Neurosci 16:71-86.

8 ABBREVIATIONS

Ab	Antibody
CaCl$_2$	Calcium chloride
CALL	Cell Adhesion molecule L1 Like
CAM	Cell Adhesion Molecule
cDNA	complementary desoxyribonucleic acid
ChAT	Choline acetyltransferase
CHL1	Close Homologue of L1
CHL1-/-	CHL1-deficient
CHL1+/+	CHL1-wild type
cm	Centimetres
cm^2	Square centimetres
cm^3	Cubic centimetres
CNPase	2´,3´-Cyclic Nucleotide 3´-Phosphodiesterase
CNS	Central Nervous System
Cy3	Cyanine 3
DH	Dorsal Horn
e.g.	exampli gratia (for example)
FGF2	Firbroblast Growth Factor 2
FN	Fibronectin
g	gram
GABA	Gamma Amino Butyric Acid
GFAP	Glial Fibrillary Acidic Protein
GM	Grey Matter
gt	genotype
i.e.	id est (that is)
Ig	Immunoglobulin
IgSF	Immunoglobulin Superfamily
i.p.	intra-peritoneal
kD	kilodalton
ko	knockout
l	litre
LTP	Long Term Potentiation
M	mole

m	metre
mg	milligram
ml	millilitre (Litre $\times 10^{-3}$)
mm	millimetre (Metre $\times 10^{-3}$)
mm^2	Square millimetres
mm^3	Cubic millimetres
n	nano (10^{-9})
NCAM	Neural Cell Adhesion Molecule
NeuN	Neuron Specific Nuclear Antigen
PCR	Polymerase Chain Reaction
PV	Parvalbumin
RT	Room Temperature
SCI	Spinal Cord Injury
SD	Standard Deviation
V	Volume
VH	Ventral Horn
v/v	volume per volume
v2	secondary visual cortex
WM	White Matter
wt	wild-type
w/v	weight per volume
ZMNH	Zentrum für Molekulare Neurobiologie Hamburg
%	Percent
3D	Three-dimensional
μ	Micro (10^{-6})
°C	Degree Celsius

9 ACKNOWLEDGEMENT / DANKSAGUNG

10 CURRICULUM VITAE

Personal Data

Date of birth	27.08.1983
Place of birth	Hamburg
Nationality	German

Education

08/1994-06/2003	Friedrich-Ebert-Gymnasium, Hamburg
08/2000-01/2004	Apprenticeship as a Chemical laboratory technician, Gymnasium Altona, Hamburg
10/2003 until now	Regular student of medicine, University of Hamburg
04/2006 until now	Doctoral candidate at Centre for Molecular Neurobiology, Hamburg

Clinical Internships

08/2006	Internship in Marienkrankenhaus, Hamburg Internal Medicine
08/2007	Internship in Great Ormond Street Hospital, London, Pediatrics
09/2007	Internship in a medical practice M. Yoldas Hamburg, General Medicine
05/2008	Internship in Avicenna Hospital, Istanbul Gynecology
08/2008-12/2008	1. PJ-Internship in Krankenhaus Buchholz, Surgery
12/2008-03/2009	2. PJ-Internship in Asklepios Klinikum Harburg, Internal Medicine
04/2009-06/2009	3. PJ-Internship in Schön Klinik Hamburg-Eilbek, Anesthesiology

Ancillary activity

06/2007-06/2008	Student assistant at the dean's office for student affairs, Medical Center Hamburg-Eppendorf, University of Hamburg

11 EIDESSTATTLICHE VERSICHERUNG

Ich versichere ausdrücklich, dass ich die Arbeit selbstständig und ohne fremde Hilfe verfasst, andere als die von mir angegebenen Quellen und Hilfsmittel nicht benutzt und die aus den benutzten Werken wörtlich oder inhaltlich entnommenen Stellen einzeln nach Ausgabe (Auflage und Jahr des Erscheinens), Band und Seite des benutzten Werkes kenntlich gemacht habe.

Ferner versichere ich, dass ich die Dissertation bisher nicht einem Fachvertreter an einer anderen Hochschule zur Überprüfung vorgelegt oder mich anderweitig um Zulassung zur Promotion beworben habe.

_____

Ayşe Acar